Accepted Manuscript

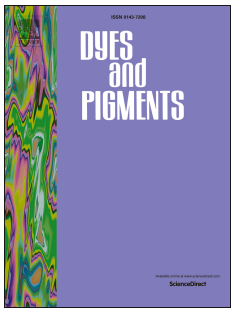

Exploration of highly efficient light conversion agents for agricultural film based on the bay-substituted perylene diimides derivatives

Yongjiang Yu, Yongtao Wang, Wenjing Liu, Xin Jia, Lei Ma, Litong Ren, Mei Xue, Xiaohong Liu

PII: S0143-7208(18)31091-X

DOI: 10.1016/j.dyepig.2018.07.015

Reference: DYPI 6869

To appear in: *Dyes and Pigments*

Received Date: 14 May 2018

Revised Date: 12 June 2018

Accepted Date: 5 July 2018

Please cite this article as: Yu Y, Wang Y, Liu W, Jia X, Ma L, Ren L, Xue M, Liu X, Exploration of highly efficient light conversion agents for agricultural film based on the bay-substituted perylene diimides derivatives, *Dyes and Pigments* (2018), doi: 10.1016/j.dyepig.2018.07.015.

This is a PDF file of an unedited manuscript that has been accepted for publication. As a service to our customers we are providing this early version of the manuscript. The manuscript will undergo copyediting, typesetting, and review of the resulting proof before it is published in its final form. Please note that during the production process errors may be discovered which could affect the content, and all legal disclaimers that apply to the journal pertain.

ACCEPTED MANUSCRIPT

Exploration of highly efficient light conversion agents for agricultural film based on the bay-substituted perylene diimides derivatives

Yongjiang Yu [a], Yongtao Wang* [ac], Wenjing Liu [a], Xin Jia* [a], Lei Ma* [b], Litong Ren [a], Mei Xue [a] and Xiaohong Liu [a]

[a]School of Chemistry and Chemical Engineering/Key Laboratory for Green Processing of Chemical Engineering of Xinjiang Bingtuan，Shihezi University，Shihezi 832003, P. R. China

[b]Tianjin International Center for Nanoparticles and Nanosystem, Tianjin University, Tianjin, 300072, P. R. China.

[c]Shenyang University of Chemical Technology

*Author for correspondence: wyt_shzu@163.com; jiaxin@shzu.edu.cn; lei.ma@tju.edu.cn

ACCEPTED MANUSCRIPT

ACCEPTED MANUSCRIPT

Abstract

To explore highly efficient yellow-green light conversion agents used for agricultural film, six bay-substituted perylene diimides and their polyvinyl chloride doped films (by 0.5% weight addition) were prepared. The maximum absorption and emission peaks of the luminogens-doped polyvinyl chloride films are located at 581-609nm and 647-667nm, respectively. More importantly, the fluorescence quantum yields of PTCDA, t-BuOPTCDA and m-MeOPTCDA are up to 0.88, 0.84 and 0.78 in doping film, respectively. The strengthening solar radiation and outdoor exposure to sunlight last 160 minutes and two months respectively and the emission intensity of m-MeOPTCDA-doped film displays slight changes and 9 percentage fluctuation in turn. Combined transmittance, compatibility, mechanical properties and thermal stability, m-MeOPTCDA is chosen as the best effective light conversion materials. To better understand the optical properties of the luminogens, molecular configuration optimization, electron cloud density distribution and molecular orbital energy levels were completed by theoretical calculation. Further, the double layer coextrusion film containing m-MeOPTCDA and Triphenyl acrylonitrile is succeed in dual band excitation (350 nm and 580 nm) and emission (430 nm and 651 nm), by optimizing the proportion of m-MeOPTCDA and Triphenyl acrylonitrile, the special light conversion films for different crops will be expected.

Keywords: photosynthesis, fluorescence, light conversion film, light conversion agents, perylene diimides.

1 Introduction

The non-renewable energy such as coal, oil and natural gas is in the danger of drying up. As a clean and renewable energy, the solar energy has been one of the research focal points of the modern agricultural science and technology [1-4]. It is well known that photosynthesis plays the most critical role in plant growth, and photosynthesis of plants heavily rely on pigments of leaves, such as chlorophyll a, b and β carotene. By absorbing the blue-violet band (400–480 nm) and red-orange band (600–700 nm) of the sunlight, the pigments conduct photosynthesis of plants[5-8]. By converting the ultraviolet (280–380 nm) light and yellow-green light (510–580 nm) of sunlight into the plant photosynthesis needs blue-violet light (400–480 nm) and red-orange light (600–700 nm), the agricultural shed film with addition of light conversion agents can improve the yield and quality of crops[9-11]. However, most of the existing light conversion agents only can convert ultraviolet light, the yellow-green light conversion

agents are not only rarely, but they are also unstable[12]. In addition, the content of ultraviolet light is only equivalent to 1%-2% of yellow-green light of the solar spectrum. Therefore, converting only 5% yellow-green can outweigh the conversion effect of whole ultraviolet light. Based on the above background, it can be deduced that it is an urgent task to explore highly efficient yellow-green light agents.

The highly efficient yellow-green light conversion agents should possess high luminescence efficiencies, excellent thermal stability, resin compatibility, weather resistance, low cost and fluorescence emission matching with crops absorption spectra. In order to guarantee the matched spectrum, the absorption spectrum of yellow-green light conversion agents should be located in the region of 510-580 nm, and the fluorescence emission peak should be near 650 nm. Obviously, the luminogens with the above characteristics are difficult to obtain. According to the literature reports, perylene diimides (PDI) have rigid planar conjugated structure, outstanding light resistance, chemical and thermal stability[13, 14], but the planar molecular configuration makes the PDI to easily form π-π packing in the solid state or doped film, leading to the fluorescence quenching[15]. In addition, PDI also suffer notorious self-absorption and solubility problems. To solve the above problem, a series of bay-substituted PDI derivatives has been designed and synthesized by Pd(0)-catalysed Suzuki cross-coupling or nucleophilic substitution reaction[16, 17]. For comparison, the 1,6, 1,7 and 1,6,7,12, bay-substituted PDI derivatives (Figure 1) show enhanced solid state fluorescence efficiency and solubility due to twisted molecular conformation[18-22]. Recently, the PDI derivatives have extended their applications

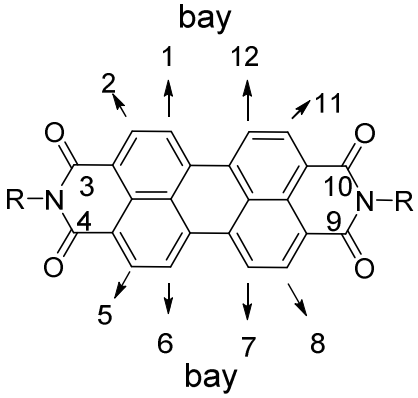

Figure 1 Perylene diimides with position numbers.

into organic photovoltaic devices[23-25], piezochromic switching[26], biological probes[27], bio-labelling[28], near-infrared fluorescence materials[29], transistors[30-32], light emitting diodes[33-34], luminescent solar concentrators[35] and so forth. However, as light conversion materials for agricultural film, the application and evaluation of bay-substituted PDI derivatives are rarely available in the literature until now.

To obtain highly efficient yellow-green light conversion agents, in this work, six different bay-substituted PDI derivatives, named PTCDA, o-MePTCDA, m-MeOPTCDA, p-MeOPTCDA, m-2MeOPTCDA, and t-BuOPTCDA, have been synthesized (As shown in Scheme 1). By the tests of photophysical properties and theoretical calculation, the structure-photophysical property relationships of the light conversion agents are analyzed and discussed in detail. Finally, the results show coextrusion film successfully achieved blue-violet (430 nm) and red-orange light (651 nm) emission, and the optimum excitation wavelength are located in ultraviolet and yellow-green light region. More importantly, the special film for different crops is expected to be completed by tuning adding proportion between PDI derivatives and Triphenylacrylonitrile(TPA).

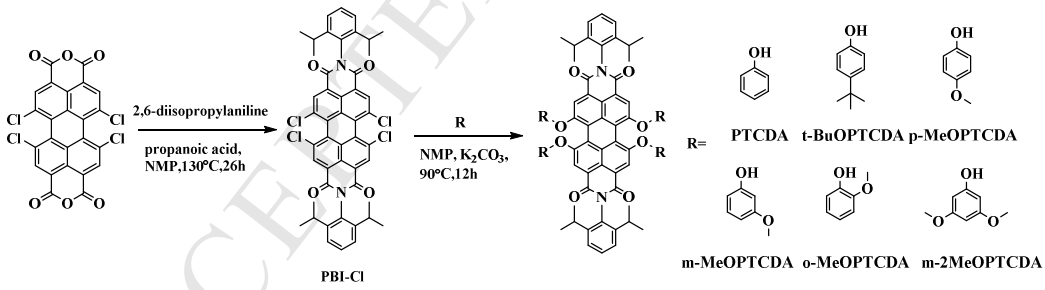

Scheme 1 Synthetic routes of PTCDA, m-2MeOPTCDA, t-BuOPTCDA, p-MeOPTCDA, o-MeOPTCDA and m-MeOPTCDA

2 Experimental Details

2.1 Measurements and characterizations

The UV-vis spectra were determined on a Mapada UV-3200pcs spectrophotometer. Fluorescence measurements were taken on Agilent Cary Eclipse fluorescence spectrophotometer. ^{1}H NMR and ^{13}C NMR spectra were obtained with a Varian inova instrument at 400 MHz and 100 MHz using tetramethylsiane (TMS) as the internal standard, and $CDCl_3$ as the solvent in all cases. MALDI/FIRMS were recorded on an Ultrafle Xtreme MALDI-TOF/TOF mass spectrometer (Bruker, Germany). Fluorescence microscopy images were obtained on OLYMPUS BX53. Photodegradation experiments were carried out by a 300W xenon lamp equipped with a filter, and radiation intensity of artificial sunlight is up to 129 mW/cm^2. Thermal stability was determined by thermogravimetric analyzer (TGA, Netzsch STA449F3) over a temperature range of 40-1000 □ at a heating rate of 20 □/min under N_2 atmosphere. The fluorescence quantum yields of PDI luminogens $CHCl_3$ solution were determined by the comparative method using *t*-BuOPTCDA ($\Phi_f = 0.72$ in $CHCl_3$) as reference[36]

2.2 Materials and Synthesis

THF, DMF and toluene were dried according to standardized procedures previously described. The synthetic method of the PBI-Cl and TPA was carried out according to the reported literature[3, 37]. All the other chemicals and reagents used in this study were of analytical grade without further purification. In general, all the intermediates and final compounds were purified by column chromatography on silica gel (200-300 mesh) while the reactions were monitored by thin-layer chromatography (TLC).

Synthesis of bis(2,6-diisopropylphenyl)-5,6,12,13-tetraphenoxyanthra[2,1,9-def:6,5,10-d'e'f']diisoquinoline-1,3,8,10(2H, 9H)-tetraone(PTCDA): PBI-Cl (1.7 g, 2 mmol) was stirred under argon with phenol (1.6 mL, 16 mmol) in N-methyl-pyrrolidone (60 mL) in a 250 mL round flask in the presence of powdered anhydrous K_2CO_3 (1.1 g, 8 mmol). The temperature was maintained at 90 □ overnight under N_2. After cooling to room

temperature, the reaction liquid was poured into the water and extracted with ethyl acetate. The combined organic layers were dried over anhydrous Na_2SO_4 and evaporated in vacuum. The crude product was purified by chromatography (silica gel, ethyl acetate: petroleum=1:10). Red solid was obtained. Yield: 92%. ^{1}H NMR (400 MHz,) δ 8.26（s, 4H）, 7.50 – 7.38 (t, 2H), 7.32 – 7.26 (m, 6H), 7.24 (d, J = 2.6 Hz, 6H), 7.09 (t, J = 7.4 Hz, 4H), 7.02 – 6.91 (m, 8H), 2.78 – 2.61 (m, 4H), 1.11 (d, J = 6.8 Hz, 24H) (Figure S6). ^{13}C NMR (101 MHz, $CDCl_3$) δ 163.17, 155.82, 155.28, 145.60, 133.17, 130.57, 129.99, 129.45, 124.59, 123.90, 122.91, 120.81, 120.39, 119.83, 29.10, 24.02 (Figure S12). LRMS (MALDI-TOF): m/z 1078.3 calculated 1078.4 (Figure S18).

Synthesis of 2,9-bis(2,6-diisopropylphenyl)-5,6,12,13-tetrakis(3,5-dimethoxyphenoxy) anthra[2,1,9-def:6,5,10-d'e'f']diisoquinoline-1,3,8,10(2H,9H)-tetraone(m-2MeOPTCDA): The compound was synthesized by the same procedure described for PTCDA using 3, 5-dimethoxyphenol and PBI-Cl, The crude product was purified by chromatography (silica gel, ethyl acetate: petroleum=1:10). Red solid was obtained. Yield: 82%. ^{1}H NMR (400 MHz, Chloroform-d) δ/ppm = 8.35 (s, 4H), 7.49-7.40 (m, 2H), 7.30 (d, J = 7.8 Hz, 4H), 6.24 (t, J = 2.2 Hz, 4H), 6.17 (d, J = 2.2 Hz, 8H), 3.66 (s, 24H), 2.72 (p, J = 6.8 Hz, 4H), 1.14 (d, J = 6.8 Hz, 24H). (Figure S7). ^{13}C NMR (100 MHz, $CDCl_3$): δ/ppm= 163.13, 161.62, 157.10, 155.32, 145.62, 133.02, 130.55, 129.49, 123.92, 122.98, 121.08, 120.78, 120.59, 98.48, 97.17, 55.40, 29.10, 24.00 (Figure S13). HRMS (MALDI-TOF): m/z 1318.5040 calculated 1318.5038 (Figure S19).

Synthesis of 5,6,12,13-tetrakis(4-(tert-butyl)phenoxy)-2,9-bis(2,6-diisopropylphenyl) anthra[2,1,9-def:6,5,10-d'e'f']diisoquinoline-1,3,8,10(2H,9H)-tetraone(t-BuOPTCDA): The compound was synthesized by the same procedure described for PTCDA using PBI-Cl and 4-(tert-butyl)phenol. The crude product was purified by chromatography (silica gel, ethyl acetate: petroleum=1:8). Red solid. Yield: 89%. ^{1}H NMR (400 MHz, Chloroform-d) δ/ppm= 8.29 (s, 4H), 7.42 (t, J = 7.8 Hz, 2H), 7.27-7.23 (m, 12H), 6.87

(d, J = 8.5 Hz, 8H), 2.77-2.65 (m, 4H), 1.28 (s, 36H), 1.13 (d, J = 6.4 Hz, 24H) (Figure S8). ^{13}C NMR (101 MHz, $CDCl_3$) δ 163.33, 155.90, 152.78, 147.33, 145.59, 133.22, 130.67, 129.37, 126.66, 123.86, 122.68, 120.75, 120.16, 119.19, 34.36, 31.44, 29.07, 24.02 (Figure S14). LRMS (MALDI-TOF): 1302.5 calculated 1302.7 (Figure S20).

Synthesis of 2,9-bis(2,6-diisopropylphenyl)-5,6,12,13-tetrakis(4-methoxyphenoxy) anthra[2,1,9-def:6,5,10-d'e'f']diisoquinoline-1,3,8,10(2H,9H)-tetraonep(p-MeOPTCD A): The compound was synthesized by the same procedure described for PTCDA using PBI-Cl and 4-methoxyphenol. The crude product was purified by chromatography (silica gel, ethyl acetate: petroleum=1:10). Red solid. Yield: 86%. ^{1}H NMR (400 MHz, Chloroform-d) δ/ppm= 8.18 (s, 4H), 7.50 -7.38 (m, 2H), 7.28 (s, 4H), 7.00-6.91 (m, 8H), 6.89- 6.77 (m, 8H), 3.79 (s, 12H), 2.69 (p, J = 6.8 Hz, 4H), 1.12 (d, J = 6.8 Hz, 24H) (Figure S9). ^{13}C NMR (101 MHz, $CDCl_3$) δ 163.28, 156.66, 156.59, 148.49, 145.61, 133.18, 130.69, 129.37, 123.84, 122.69, 121.33, 120.17, 119.92, 119.30, 115.20, 55.71, 29.08, 24.03 (Figure S15). LRMS (MALDI-TOF): 1198.4 (Figure S21).

Synthesis of 2,9-bis(2, 6-diisopropylphenyl)-5,6,12,13-tetrakis(2-methoxyphenoxy) anthra[2,1,9-def:6,5,10-d'e'f']diisoquinoline-1,3,8,10(2H,9H)-tetraone(o-MeOPTCDA): The compound was synthesized by the same procedure described for PTCDA using PBI-Cl and 4-(tert-butyl)phenol The crude product was purified by chromatography (silica gel, ethyl acetate: petroleum=1:8). Red solid. Yield: 81%. ^{1}H NMR (400 MHz, Chloroform-d) δ/ppm= 8.10 (s, 4H), 7.44-7.37 (m, 2H), 7.27-7.25 (m, 4H), 7.11-7.03 (m, 8H), 6.90 (dd, J = 8.2, 1.2 Hz, 4H), 6.80 (td, J = 7.9, 1.4 Hz, 4H), 3.66 (s, 12H), 2.70 (p, J = 6.8 Hz, 4H), 1.12 (d, J = 6.8 Hz, 24H) (Figure S10). ^{13}C NMR (101 MHz, $CDCl_3$) δ 163.56, 155.94, 151.13, 145.65, 143.22, 133.41, 130.90, 129.29, 125.74, 123.81, 122.35, 121.84, 121.16, 120.02, 120.00, 118.73, 112.50, 55.50, 29.08, 23.96 (Figure S16). LRMS (MALDI-TOF): 1198.4 (Figure S22)

Synthesis of 2,9-bis(2,6-diisopropylphenyl)-5,6,12,13-tetrakis(3-methoxyphenoxy) anthra[2,1,9-def:6,5,10-d'e'f']diisoquinoline-1,3,8,10(2H,9H)-tetraone(m-MeOPTCDA): The compound was synthesized by the same procedure described for PTCDA using PBI-Cl and 4-(tert-butyl)phenol The crude product was purified by chromatography (silica gel, ethyl acetate: petroleum=1:10). Red solid. Yield: 85%. ^{1}H NMR (400 MHz, Chloroform-d) δ/ppm= 8.31 (s, 4H), 7.44 (t, J = 7.7 Hz, 2H), 7.29 (d, J = 7.8 Hz, 4H), 7.19 (t, J = 8.2 Hz, 4H), 6.68 (dd, J = 8.3, 2.3 Hz, 4H), 6.61 (dd, J = 8.1, 2.1 Hz, 4H), 6.53 (t, J = 2.3 Hz, 4H), 3.67 (s, 12H), 2.72 (p, J = 6.9 Hz, 4H), 1.13 (d, J = 6.8 Hz, 24H) (Figure S11). ^{13}C NMR (101 MHz, $CDCl_3$) δ 163.15, 161.02, 156.38, 155.60, 145.61, 130.57, 130.38, 129.47, 123.91, 122.95, 120.75, 120.69, 120.47, 111.96, 110.72, 105.85, 55.36, 29.10, 24.02 (Figure S17). LRMS (MALDI-TOF): 1198.4 (Figure S23)

2.3 Preparation of light conversion films

Polyvinyl chloride (PVC) (2.4725 g) and PTCDA (0.0125 g) were dissolved into 16 mL THF in a mechanical stirrer containing single drying flask. The mixture was stirred for 12 h at room temperature and placed in the ultrasonic oscillator for 30 minutes to remove the bubbles from the mixture. The mixture was poured onto a glass plate and paved rapidly with a glass rod. Finally, the mixture was placed into ventilated cabinets until THF volatilized completely, and light conversion film of PTCDA (0.5% mass fraction) was obtained in this way. The other light conversion films were prepared according to the same method. The composite light conversion films were prepared by tuning weight ratio of TPA (the weight ratio of TPA: m-MeOPTCDA=1:1, 2:1 and 4:1, and maintain 0.5% weight ratio between PDI derivatives and PVC).

3 Results and Discussion

3.1 Photo-physical properties in solutions and PVC film

ACCEPTED MANUSCRIPT

To analyze the impact of various bay position substituents, the UV-vis absorption spectra and fluorescence emission spectra of six PDI derivatives have been investigated in different polar solvents. As shown in Figure S1 and Table S1, in addition to the ultraviolet region, the PDI dyes exhibit three absorption bands ranging from 400 to 630 nm, the corresponding absorption peaks are located near 450, 540 and 570 nm, respectively. Furthermore, the broad peak at 450 nm and the shoulder peak at 540 nm are assigned to the S_0–S_2 transition, while the strongest absorption peak at 570 nm is related to the S_0–S_1 transition[38]. With the increase of solvent polarity, the maximum absorption peak (TMAP) between toluene and THF shows abnormal shift due to solvation effect of toluene, which leads to extended molecular conjugation. Generally, TMAP of the PDI dyes only exhibits less than 10 nm shift with the change of polarity of solvent, which shows that the polarity of solvent has little influence on the ground state energy level. Compared with steric substituent effects, the electron donating ability of substituents has notable influence on electron delocalization. Taking p-MeOPTCDA as an example, the maximum absorption peak shows the most obvious redshift in THF and DMF due to the stronger electron donating ability of p-MeO group. Similar to absorption spectra, the maximum fluorescence emission peak of the dyes also exhibit tiny shift (19 nm at most) with the change of solvent polarity and substituent. To screen the best yellow-green light conversion agent, the excitation and emission spectra of PVC films doped PDI dyes are tested. As shown in Figure S2 and Table S2, the maximum excitation and emission peak are located at 581-609 nm and 651-667 nm, respectively. Obviously, larger stokes shifts are desirable for decreasing of re-absorption of emission, and the red-shifted fluorescence emission peaks match well with the absorption spectrum of crops in the region of red-orange light. Combined with the excitation spectra, PTCDA and m-MeOPTCDA are the most appropriate yellow-green light conversion materials in the PDI luminogens. The maximum excitation and emission peak of PTCDA and m-MeOPTCDA are located at 581 nm and 651 nm, respectively. Although the excitation peak of two dyes slightly exceeds the optimum region of 510-580 nm, asymmetric curve of the excitation spectra is in favor of offsetting it. More interesting,

PDI luminogens containing -OMe group show the smaller width of the half peak (FWHM) than that of PTCDA and *t*-BuOPTCDA. Based on the preliminary study, the bigger FWHF often means poor uniformity of crystal particles or amorphous states. Thus, we speculate that the presence of -OMe group is beneficial to improve crystallization properties of PDI dyes. To better understand the optical characteristics of the PDI dyes, frontier molecular orbital analysis of the luminogens was performed by using density functional theory (DFT) at the B3LYP/6-31G(d,p) level. As shown in Figure 2, the electron clouds in both the highest occupied molecular orbital (HOMO) level and the lowest unoccupied molecular orbital (LUMO) level are all predominantly placed on the PDI unit, while only tiny amounts of HOMO

ACCEPTED MANUSCRIPT

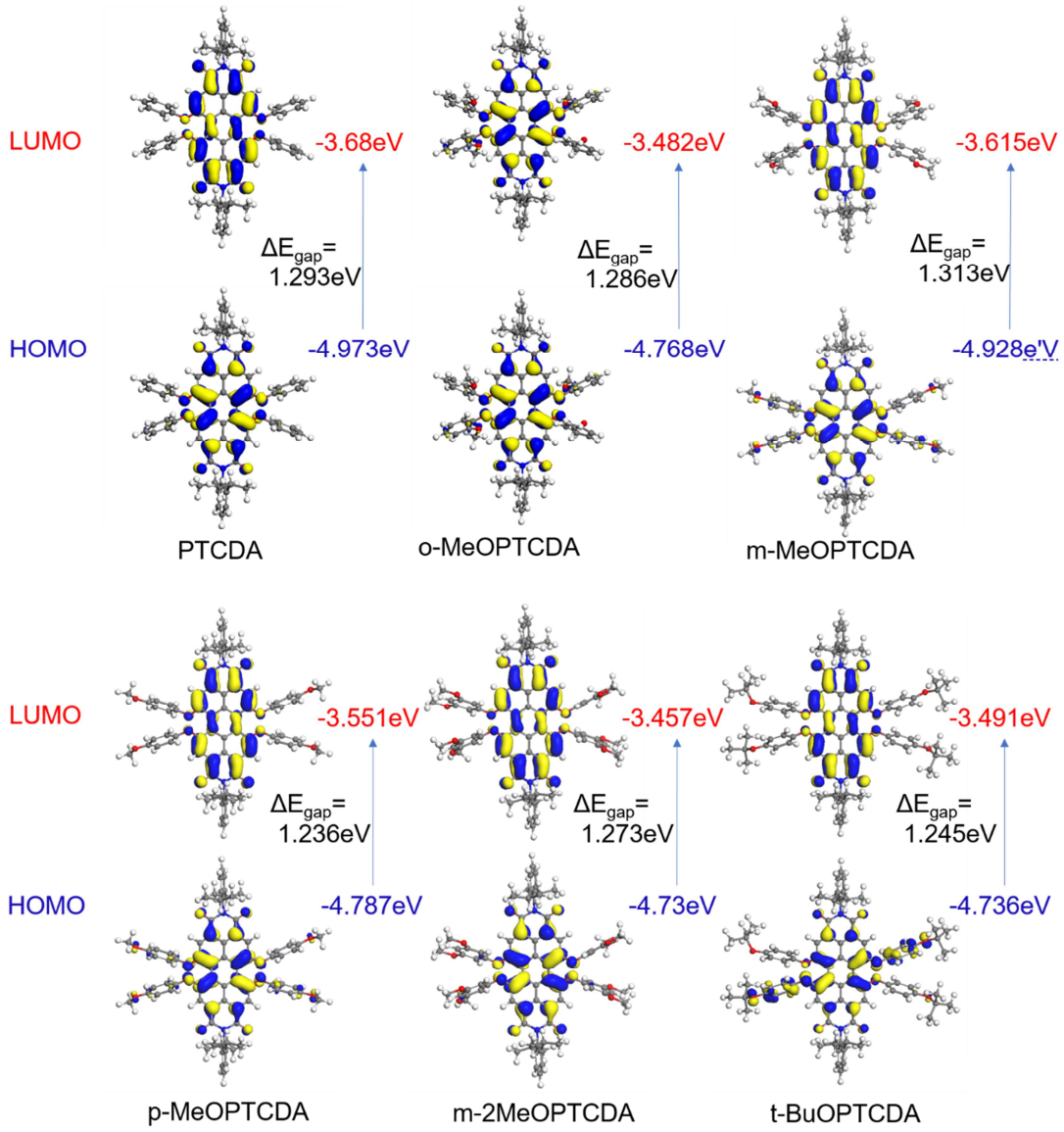

Figure 2 B3LYP/6-31G(d,p) calculated molecular orbital amplitude plots of HOMO and LUMO levels for PTCDA, o-MeOPTCDA, m-MeOPTCDA, p-MeOPTCDA, m-2MeOPTCDA and t-BuOPTCDA.

levels extend to the bay-substituted aryl oxygen unit, indicative of faint intramolecular charge transfer (ICT) characteristic in the molecules in accordance with spectroscopic results. Compared with PTCDA, the HOMOs and LUMOs of the other bay-substituted PDI compounds showed upshift more obviously due to the electron-donating properties of $–OCH_3$ and $–O\mathit{t}C_4H_9$ groups. However, the energy gaps of PDI derivatives were irregular. In addition to increased MeOPTCDA, the energy gaps of luminogens including o-MeOPTCDA, p-MeOPTCDA, m-2MeOPTCDA and *t*-BuOPTCDA were smaller than PTCDA (Figure 2), which

means that the alkoxy substituents with different type, position and amount can cause varying degrees of change of the HOMOs and LUMOs. In addition to the electron-donor ability of alkoxy groups, molecular conformation and packing also affect optical characteristics of luminogens. Because of the stronger electron-donor ability, the maximum excitation and emission peaks of p-MeOPTCDA and *t*-BuOPTCDA are longer than that of the other compounds in the doping films, (Table S2), while m-MeOPTCDA show blue-shifted maximum excitation and emission peaks. Specially, m-2MeOPTCDA exhibited the shortest fluorescence emission peak among the PDI dyes, which can be attributed to twisted PDI core and further

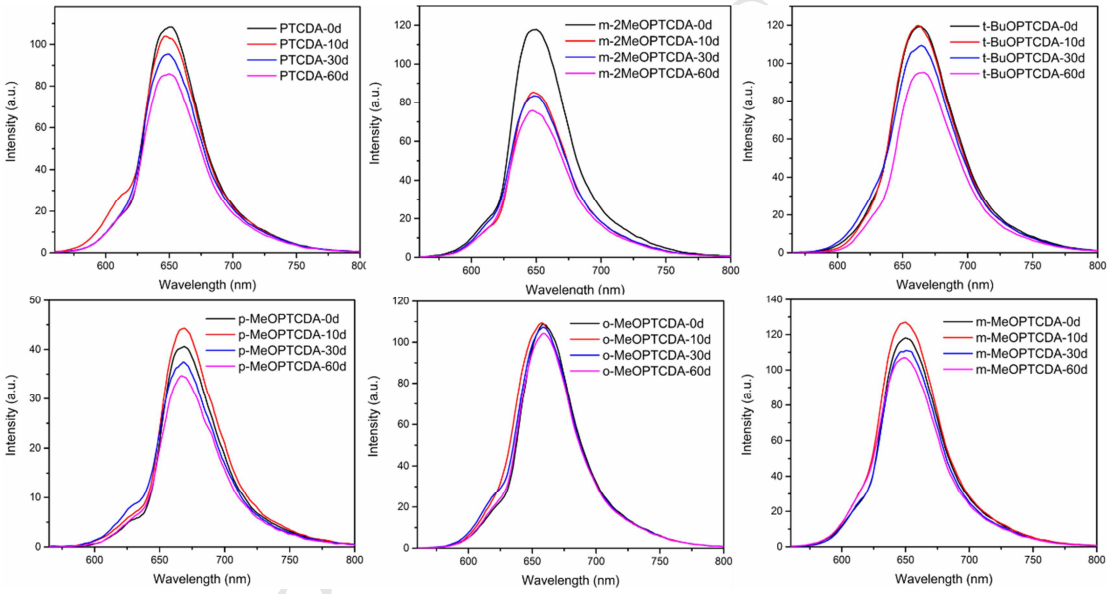

Figure 3 The fluorescence spectra of PDI luminogens in PVC films under sunlight for different days

explanation will be given in the following section.

In order to investigate the photostability of light conversion agents, the test of strengthening solar radiation is essential. Under strengthening solar radiation (129 mW/cm^2), the fluorescence emission intensity of the doping films is evaluated at different times. As shown in Figure S3, after 160 minutes, the fluorescence intensity of o-MeOPTCDA and p-MeOPTCDA displays slight fluctuation, but, quite apart from that, continuous radiation has almost no influence on the remaining PDI luminogens. To further evaluate practical application performance of PDI luminogens,

the fluorescent intensity of the doping films are investigated after outdoor exposure to sunlight for two months. The o-MeOPTCDA film shows some minor differences, for m-MeOPTCDA film, 91% of the initial intensity is reserved, and the shape and shift of emission peaks are unchanged. As shown in Figure 3, the above results indicate o-MeOPTCDA and m-MeOPTCDA have excellent weather resistance. However, the initial fluorescence emission intensity of the luminogens are significantly different. Among of them, fluorescence emission of p-MeOPTCDA is the weakest, while PTCDA and m-MeOPTCDA exhibit the strongest fluorescence emission under excitation of the same wavelength, which means PTCDA and m-MeOPTCDA may have higher fluorescence quantum efficiency than the others. According to the literature report[39], the aryloxy bay substituents and PDI core act as electron donator and electron acceptor in bay-substituted PDI derivative, respectively, while fluorescence quantum efficiency depend on ICT effect from electron donor to electron acceptor. In addition, the ICT effect is related to the dihedral angles between the aryloxy groups and the PDI core as well as the angle of the oxygen lone pair orbitals relative to the π-orbitals of the PDI core. However, the opposite trends of the two angles lead to irregularand unpredictable ICT effects. Different from the literature reports, the PDI core is twisted into two naphthalimide planes A and B, and dihedral angle of the two planes should be a significant influencing factors on ICT effects. For comparison, PTCDA, m-MeOPTCDA and m-2MeOPTCDA have bigger dihedral angle between plane A and B based on molecular structure optimization (As shown in Figure 4), leading to diminished ICT effects and blue-shifted fluorescence emission. Meanwhile, the twisted PDI core is conducive to decrease π-π stacking and improve the solid-state fluorescence quantum efficiency, which is suitable for PTCDA and m-MeOPTCDA possessing higher fluorescence quantum efficiency than the others, but does nothing for explaining fluorescence quenching of m-2MeOPTCDA. In general, the alkoxy substituents on benzene ring in bay position is not beneficial to the improvement of solid-state fluorescence efficiency. In addition to ICT effect and twisted PDI core, obtaining molecular arrangement and stacking mode may give a better explanation. Next, we tried to cultivate single crystals of the compounds, but

failed. Compared with the fluorescence quantum efficiency in solution and solid state, the PVC doped films exhibit significantly enhanced fluorescence emission due to doping and dilution effect,

ACCEPTED MANUSCRIPT

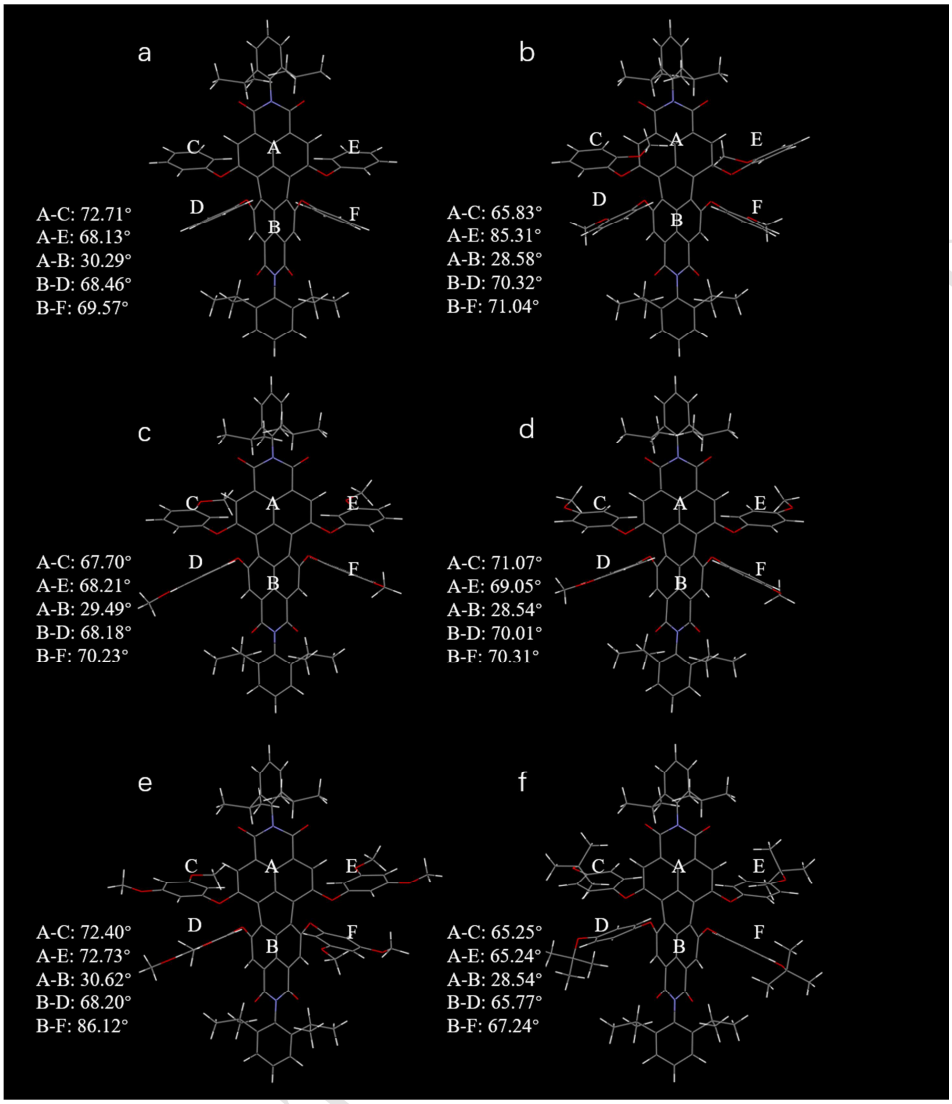

Figure 4 B3LYP/6-31G(d,p) calculated molecular structure of PTCDA(a), o-MeOPTCDA(b), m-MeOPTCDA(c), p-MeOPTCDA(d), m-2MeOPTCDA(e) and t-BuOPTCDA(f).

especially, fluorescence quantum yields of PTCDA, *t*-BuOPTCDA and m-MeOPTCDA are up to 0.88, 0.84 and 0.78 respectively(Figure 5). Based on theoretical calculation, *t*-BuOPTCDA has the best plane configuration generally deteriorating the fluorescence properties of the solid state and doping films, so high fluorescence quantum yields of *t*-BuOPTCDA should be attributed to the steric effect of tert-butyl reducing intermolecular interactions. Obviously, the fluorescence quantum yields of doping films cannot be simply sorted only by solid state quantum yields of luminogens, for instance, *t*-BuOPTCDA. More importantly, the twisted

degree of PDI core and large *t*-BuO group will provide theoretical guidance for

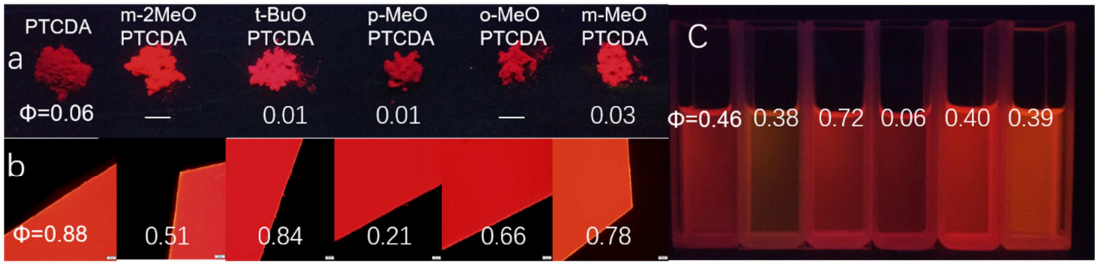

further molecular design of light conversion agents.

Figure 5 The Fluorescence quantum efficiency of PDI luminogens: a) solid state, b) in PVC films, c) in solution ($1x10^{-5}$mol/L, $CHCl_3$), from left to right: PTCDA, m-2MeOPTCDA, t-BuOPTCDA, p-MeOPTCDA, o-MeOPTCDA, m-MeOPTCDA. c) PVC films.

3.2 UV-visible transmittance analysis, compatibility and dispersibility of light conversion films

Based on performance evaluation of light conversion agents, it is necessary to test the transmittance curves of doping films. Taking PVC film as reference, the transmittance of different wavebands is calculated by integrating the area of transmittance curve. As shown in Figure 6 and Table S3, the transmittance curve indicates that there are different degrees of decline in the whole UV-vis range. For the doping films, the dominant light conversion regions are still yellow-green and ultraviolet lights. Especially, only less than 30% yellow-green light can penetrate through the doping films. Next to yellow-green light, the transmittance of ultraviolet light is lower than 50%. Compared to yellow green and ultraviolet light, the conversion of blue-violet and red-orange light (600-650 nm) is not expected. Fortunately, PTCDA and m-MeOPTCDA give about 90% transmittance in the region of 600-650 nm. Moreover, the films doped with light conversion agents have almost no influence on transmittance of the red-orange light (650–700 nm), which should be attributed to the good compatibility and dispersibility between the PDI dyes and PVC matrix (Figure 5b).

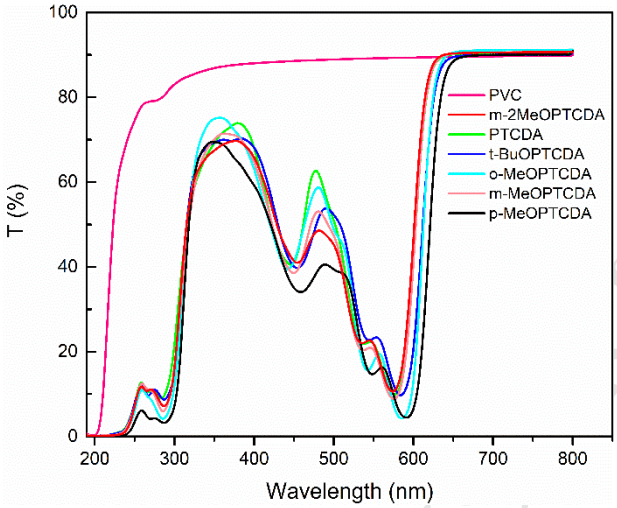

Figure 6 UV-visible transmittance spectra of PTCDA(a), t-BuOPTCDA(b), o-MeOPTCDA(c), m-MeOPTCDA(d), p-MeOPTCDA(e) and m-2MeOPTCDA(f) in PVC films and blank PVC film.

Mechanical properties of light conversion films

Referring to national standard (GB/13022-91), mechanical properties of the doping films were tested at stretching speed of 10 mm min^{-1}. Taking advantage of millesima thickness gauge/AICE, the thickness of the light conversion films was tested and calculated by averaging the testing values of five random test points. As shown in Table 1, the data indicates that PTCDA film exhibits the worst tensile stress, but apparent substitution effects are found in terms of tensile stress. Compared with PVC film, tensile stress of the other doping films are improved by nearly 30%. Contrary to tensile stress, it is difficult to find a clear regularity between the structure of PDI luminogens and elongation. Among them, p-MeOPTCDA film exhibits the best elasticity, followed by the PTCDA, m-2MeOPTCDA, m-MeOPTCDA, o-MeOPTCDA and *t*-BuOPTCDA, while *t*-BuOPTCDA film suffers from a slight decrease compare to PVC film. The large steric hindrance of *t*-Bu may be detrimental to formation of intermolecular hydrogen interactions reducing elasticity of *t*-BuOPTCDA.

Table 1 Mechanical properties of light conversion films.

Entry	Tensile stress (Mpa)	Elongation (%)	Thickness (mm)
	Transverse/Portrait	Transverse/Portrait	
PVC	33.13/31.20	13.50/12.49	0.053
PTCDA	24.03/24.03	40.12/41.09	0.050
m-2MeOPTCDA	44.23/48.52	33.71/33.20	0.053
t-BuOPTCDA	42.07/41.87	11.53/11.37	0.054
p-MeOPTCDA	43.53/49.89	101.97/88.05	0.047
o-MeOPTCDA	38.55/47.94	20.09/13.01	0.056
m-MeOPTCDA	43.27/48.58	57.11/19.90	0.050

3.3 Thermal stability

By the comparing the performance of the light conversion agents and their doping films, PTCDA and m-MeOPTCDA have been appointed as the highly efficient yellow-green light conversion agents. However, thermal stability of the light conversion agents is an important evaluating indicator. As an ultimate showdown between PTCDA and m-MeOPTCDA, thermal gravimetric analysis (TGA) are observed. The thermal decomposition of PTCDA and m-MeOPTCDA can be divided into two stages. The initial decomposition temperatures of PTCDA and m-MeOPTCDA are 103 ˚C and 198 ˚C respectively, according to weight loss, the bay-substituted benzene and MeO- may be removed in the first stage. In addition, PTCDA shows a faster decomposition rate than m-MeOPTCDA, presenting as a tilted line in the range of 100 ˚C. The second stages occur between 400 ˚C and 600 ˚C, this rapid decomposition should be the result of decomposition, oxidation and combustion. Generally, PTCDA and m-MeOPTCDA can meet the application requirements of light conversion agents, but the higher initial decomposition temperature and up to 493 ˚C T_d (defined as the temperature at which a sample loses its 5% weight) indicate that m-MeOPTCDA has excellent thermal stability (Figure 7).

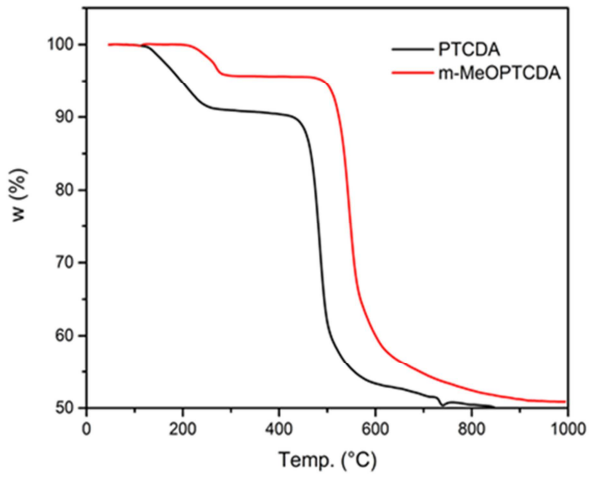

Figure 7 TGA thermograms of PTCDA(a) and m-MeOPTCDA(d) recorded under nitrogen atmosphere at 10 ℃min^{-1} scan rates

The composite and the double layer coextrusion film containing m-MeOPTCDA and TPA

Some crops prefer red-orange light compared with blue-violet light, but some crops are just the opposite. Unfortunately, the excitation intensity scopes of m-MeOPTCDA cover the blue-violet region. To reduce the adverse effect of blue-violet light absorption as well as meet requirements of different crops, the tunable dual-band light conversion films will become a development tend in the future. By tuning the adding proportion of m-MeOPTCDA and TPA, the transmittance curves of composite films are investigated. As shown in Figure S4 and Table S4, relative to the doping film of single light conversion agent, the composite films obviously reduce transmittance of ultraviolet light, and accompanied by increasing transmittance of blue-violet light and yellow-green light. With the increasing of TPA, transmittance curve of the doping film reveals tiny change in the blue-violet and the yellow-green region compared to equal weight addition of TPA and m-MeOPTCDA. Compared with m-MeOPTCDA film, fluorescence emission intensity of composite films reduced after the first increase by UV light excitation. When the weight addition of m-MeOPTCDA and TPA is 1:1 or 1:2, the enhanced red-orange light emission is obvious, however, the

luminescence intensity decreases rapidly when the addition ratio of m-MeOPTCDA and TPA is 1:4, which means that π-π interactions may occur. Unfortunately, the fluorescence emission of all the composite films is almost imperceptible in the blue-violet light region (As shown in Figure S5). Based on the above investigation, a conclusion can be drawn that the addition of TPA may enhance emission intensity of red orange light but do nothing to obtain dual band light conversion film, which is attributed to Förster energy transfer from TPA to m-MeOPTCDA. To eliminate side effects of the energy transfer, the double layer coextrusion film containing TPA and m-MeOPTCDA layers is prepared. Meanwhile, taking m-MeOPTCDA layer as outer layer avoids absorbing blue-violet light from TPA layer. As expected, the bilayer film is succeed in dual band excitation and emission (As shown in Figure 8). In addition, the special light conversion films for different crops are expected to be prepared by

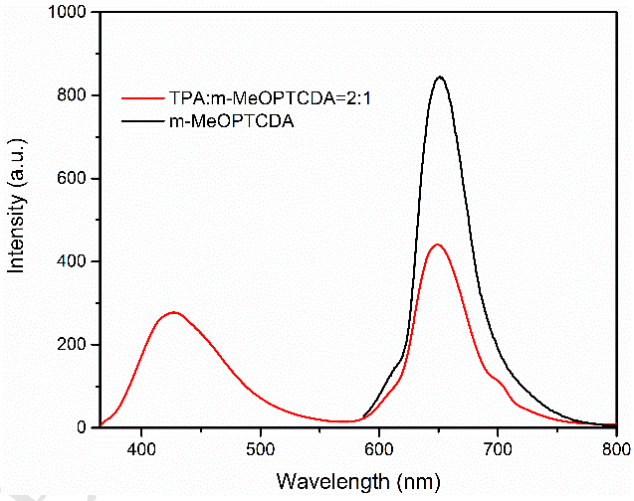

Figure 8 The fluorescence spectra of double layer coextrusion (red line, λex=350 nm) and m-MeOPTCDA film (black line, λex=550 nm)

changing addition ratio of different light conversion agents.

4 Conclusion

In summary, a series of yellow-green light conversion agents for agricultural film based on bay-substituted PDI dyes were successfully prepared after two steps of reaction. The PDI fluorophores suffer from aggregation induced fluorescence quenching problem, but exhibit enhanced fluorescence emission properties in PVC

doped film. Especially for PTCDA, *t*-BuOPTCDA and m-MeOPTCDA, the fluorescence quantum yields are up to 0.88, 0.84 and 0.78 respectively. The excellent fluorescence property is attributed to dilution effect and restrained vibration and rotation coming from polymer matrix, decreasing intermolecular interaction by large substituent groups and twisted PDI core. Meanwhile, m-MeOPTCDA shows remarkable photo stability, and the fluorescence emission intensity of the doping film displays slight changes by strengthening solar radiation (129 mW/cm^2) for 160 minutes, and fluctuates within the range of 9 percentage after outdoor exposure to sunlight for two months. The comprehensive evaluation of the doping film in terms of such aspects as optical characteristics, mechanical properties and thermal stability indicate m-MeOPTCDA is the best light conversion agent among of the PDI luminogens. The light conversion film doped m-MeOPTCDA not only emit matched fluorescence (651 nm) with absorption spectra of crops, but also maintain transmittance of 45% ultraviolet light and 25% yellow-green at 0.5wt% compared to the blank PVC film, which means ultraviolet light and yellow-green light can be converted effectively by m-MeOPTCDA, the results indicate that m-MeOPTCDA has practical application value as light conversion agent used for agricultural film. Based on the optical properties of the composite and double layer coextrusion film containing m-MeOPTCDA and TPA, the composite film cannot achieve dual band emission due to energy transfer between m-MeOPTCDA and TPA, while blue-violet and red-orange light emission can be detected simultaneously from the double layer coextrusion film by ultraviolet excitation, meanwhile, single red-orange light emission can be detected by yellow-green excitation, which will provide an effective way to obtain the special light conversion films for different crops by tuning the addition ratio of m-MeOPTCDA and TPA.

Acknowledgements

This work was supported by the National Natural Science Foundation of China (Grant Nos. 21766030, 21566034，11774255), the key program of Natural Science

Foundation of Tianjin (Grant Nos.17JCZDJC30100), the Seed Program of Tianjin University (Grant Nos. 2017XZC-0090). This paper is completed under the guidance of associate professor Yongtao Wang, and theoretical calculation are provided by Professor Lei Ma.

References

[1] Briassoulis D, Aristopoulou A, Bonora M, Verlodt I. Degradation Characterisation of Agricultural Low-density Polyethylene Films. Biosys Eng. 2004;88(2):131-143.

[2] Gu Y-J, Yan B, Qiao X-F. Novel light-conversion hybrids of SBA-16 functionalized with rare earth (Eu^{3+}, Nd^{3+}, Yb^{3+}) complexes of modified 2-methyl-9-hydroxyphenalenone and 1,10-phenanthroline. J Solid State Chem. 2013;199:116-122.

[3] Qi Y, Wang Y, Yu Y, Liu Z, Zhang Y, Qi Y, et al. Exploring highly efficient light conversion agents for agricultural film based on aggregation induced emission effects. J Mater Chem C. 2016;4(47):11291-11297.

[4] Dang S, Yu J-B, Wang X-F, Guo Z-Y, Sun L-N, Deng R-P, et al. A study on the NIR-luminescence emitted from ternary lanthanide [Er(III), Nd(III) and Yb(III)] complexes containing fluorinated-ligand and 4,5-diazafluoren-9-one. J Photochem Photobiol A: Chem. 2010;214(2-3):152-160.

[5] Björkman O. Further Studies on Differentiation of Photosynthetic Properties in Sun and Shade Ecotypes of Solidago virgaurea. Physiol Plant. 1968;21(1):84-99.

[6] Lüning K, Dring MJ. Action spectra and spectral quantum yield of photosynthesis in marine macroalgae with thin and thick thalli. Mar Biol. 1985;87(2):119-129.

[7] Korbee N, Figueroa FL, Aguilera J. Effect of light quality on the accumulation of photosynthetic pigments, proteins and mycosporine-like amino acids in the red alga Porphyra leucosticta (Bangiales, Rhodophyta). J Photochem Photobiol B: Biol. 2005;80(2):71-78.

[8] Thwe AA, Kim YB, Li X, Seo JM, Kim SJ, Suzuki T, et al. Effects of light-emitting diodes on expression of phenylpropanoid biosynthetic genes and accumulation of phenylpropanoids in Fagopyrum tataricum sprouts. J Agric Food Chem. 2014;62(21):4839-4845.

[9] Liu D, Wang Z. Novel polyaryletherketones bearing pendant carboxyl groups and their rare earth complexes, Part I: Synthesis and characterization. Polymer. 2008;49(23):4960-4967.

[10] Oxley DS, Walters RW, Copenhafer JE, Meyer TY, Petoud Sp, Edenborn HM. Mono- and Terfluorene Oligomers as Versatile Sensitizers for the Luminescent Eu3+Cation. Inorg Chem. 2009;48(14):6332-63344.

[11] Engelen-Eigles G, Holden G, Cohen JD, Gardner G. The Effect of Temperature, Photoperiod, and Light Quality on Gluconasturtiin Concentration in Watercress (Nasturtium officinale R. Br.). J Agric Food Chem. 2006;54(2):328-334.

[12] Stabilizing agricultural films: a question of balance. Plastics, Additives and Compounding. 2003;5(4):20-23.

[13] Kamm V, Battagliarin G, Howard IA, Pisula W, Mavrinskiy A, Li C, et al. Polythiophene:Perylene Diimide Solar Cells – the Impact of Alkyl-Substitution on the Photovoltaic Performance. Advanced Energy Materials. 2011;1(2):297-302.

[14] Shin WS, Jeong H-H, Kim M-K, Jin S-H, Kim M-R, Lee J-K, et al. Effects of functional groups at perylene diimide derivatives on organic photovoltaic device application. J Mater Chem. 2006;16(4):384-390.

[15] Heek T, Fasting C, Rest C, Zhang X, Würthner F, Haag R. Highly fluorescent water-soluble polyglycerol-dendronized perylene bisimide dyes. Chem Commun. 2010;46(11):1884.

[16] Shoaee S, An Z, Zhang X, Barlow S, Marder SR, Duffy W, et al. Charge photogeneration in polythiophene-perylene diimide blend films. Chem Commun. 2009(36):5445-5447.

[17] Mizoshita N, Goto Y, Maegawa Y, Tani T, Inagaki S. Tetraphenylpyrene-Bridged Periodic Mesostructured Organosilica Films with Efficient Visible-Light Emission. Chem Mater. 2010;22(8):2548-2554.

[18] Dinçalp H, Çimen O, Ameri T, Brabec CJ, İçli S. Synthesis, characterization and optoelectronic properties of a new perylene diimide–benzimidazole type solar light harvesting dye. Spectrochimica Acta Part A: Molecular and Biomolecular Spectroscopy. 2014;128:197-206.

[19] Geng Y, Li H-B, Wu S-X, Su Z-M. The interplay of intermolecular interactions, packing motifs and electron transport properties in perylene diimide related materials: a theoretical perspective. J Mater Chem. 2012;22(39):20840.

[20] ter Schiphorst J, Kendhale AM, Debije MG, Menelaou C, Herz LM, Schenning APHJ. Dichroic Perylene Bisimide Triad Displaying Energy Transfer in Switchable Luminescent Solar Concentrators. Chem Mater. 2014;26(13):3876-2878.

[21] Dinçalp H, Kızılok Ş, İçli S. Fluorescent macromolecular perylene diimides containing pyrene or indole units in bay positions. Dyes and Pigments. 2010;86(1):32-41.

[22] Xie N-H, Li C, Liu J-X, Gong W-L, Tang BZ, Li G, et al. The synthesis and aggregation-induced near-infrared emission of terrylenediimide–tetraphenylethene dyads. Chem Commun. 2016;52(34):5808-5811.

[23] Lee H-Y, Huang H-L. Performance improvement of pentacene-doped P3HT:PCBM inverted polymer solar cells with AZO nanorod array passivated using photoelectrochemical technique. Org Electron. 2014;15(7):1362-1367.

[24] Kozma E, Kotowski D, Catellani M, Luzzati S, Cavazzini M, Bossi A, et al. Design of perylene diimides for organic solar cell: Effect of molecular steric hindrance and extended conjugation. Mater Chem Phys. 2015;163:152-160.

[25] Rajaram S, Armstrong PB, Kim BJ, Fréchet JMJ. Effect of Addition of a Diblock Copolymer on Blend Morphology and Performance of Poly(3-hexylthiophene):Perylene Diimide Solar Cells. Chem Mater. 2009;21(9):1775-1777.

[26] Liu Y, Li YJ, Jiang L, Gan HY, Liu HB, Li YL, et al. Assembly and characterization of novel hydrogen-bond-induced nanoscale rods. J Org Chem. 2004;69(26):9049-9054.

[27] Abdalla MA, Bayer J, Rädler JO, Müllen K. Synthese und Selbstorganisation von Perylendiimid-Oligonucleotid-Konjugaten. Angew Chem. 2004;116(30):4057-4060.

[28] Yang SK, Shi X, Park S, Doganay S, Ha T, Zimmerman SC. Monovalent, Clickable, Uncharged, Water-Soluble Perylenediimide-Cored Dendrimers for Target-Specific Fluorescent Biolabeling. J Am Chem Soc. 2011;133(26):9964-9967.

[29] Nisha SK, Asha SK. Random Copolyesters Containing Perylene Bisimide: Flexible Films and Fluorescent Fibers. ACS Applied Materials & Interfaces. 2014;6(15):12457-12466.

[30] Zhan X, Tan Za, Domercq B, An Z, Zhang X, Barlow S, et al. A High-Mobility Electron-Transport Polymer with Broad Absorption and Its Use in Field-Effect Transistors and

ACCEPTED MANUSCRIPT

All-Polymer Solar Cells. J Am Chem Soc. 2007;129(23):7246-7247.

[31] Gao X, Hu Y. Development of n-type organic semiconductors for thin film transistors: a viewpoint of molecular design. Journal of Materials Chemistry C. 2014;2(17):3099-117.

[32] Chen S, Chen G, Ratner MA. Designing Principles of Molecular Quantum Interference Effect Transistors. J Phys Chem Lett. 2018;9(11):2843-2847.

[33] Gupta RK, Ulla H, Satyanarayan MN, Sudhakar AA. A Perylene-Triazine-Based Star-Shaped Green Light Emitter for Organic Light Emitting Diodes. Eur J Org Chem. 2018;2018(13):1608-1613.

[34] Ego C, Marsitzky D, Becker S, Zhang J, Grimsdale AC, Müllen K, et al. Attaching Perylene Dyes to Polyfluorene: Three Simple, Efficient Methods for Facile Color Tuning of Light-Emitting Polymers. J Am Chem Soc. 2003;125(2):437-443.

[35] Sadrai M, Hadel L, Sauers RR, Husain S, Krogh-Jespersen K, Westbrook JD, et al. Lasing action in a family of perylene derivatives: singlet absorption and emission spectra, triplet absorption and oxygen quenching constants, and molecular mechanics and semiempirical molecular orbital calculations. The Journal of Physical Chemistry. 1992;96(20):7988-7996.

[36] Dubey RK, Westerveld N, Sudhölter EJR, Grozema FC, Jager WF. Novel derivatives of 1,6,7,12-tetrachloroperylene-3,4,9,10-tetracarboxylic acid: synthesis, electrochemical and optical properties. Org Chem Front. 2016;3(11):1481-1492.

[37] Scheinhardt B, Trzaskowski J, Baier MC, Stempfle B, Oppermann A, Wöll D, et al. Anisotropic Polyethylene Nanocrystals Labeled with a Single Fluorescent Dye Molecule: Toward Monitoring of Nanoparticle Orientation. Macromolecules. 2013;46(19):7902-7910.

[38] Banert K, Hagedorn M, Pester T, Siebert N, Staude C, Tchernook I, et al. Rearrangement Reactions of Tritylcarbenes: Surprising Ring Expansion and Computational Investigation. Chemistry - A European Journal. 2015;21(42):14911-14923.

[39] Osswald P, Würthner F. Conformational Effects of Bay Substituents on Optical, Electrochemical and Dynamic Properties of Perylene Bisimides: Macrocyclic Derivatives as Effective Probes. Chemistry - A European Journal. 2007;13(26):7395-7409.

ACCEPTED MANUSCRIPT

ACCEPTED MANUSCRIPT

Supporting Information For: Exploration of highly efficient light conversion agents for agricultural film based on the bay-substituted perylene diimides derivatives

Yongjiang Yu [a], Yongtao Wang* [ac], Wenjing Liu [a], Xin Jia* [a], Lei Ma* [b], Litong Ren [a], Mei Xue [a]and Xiaohong Liu [a]

[a]School of Chemistry and Chemical Engineering/Key Laboratory for Green Processing of Chemical Engineering of Xinjiang Bingtuan, Shihezi University, Shihezi 832003, Xinjiang, P. R. China.

[b]Tianjin International Center of Nanoparticles and Nanosystem, Tianjin University, Tianjin, 300072, P. R. China.

[c]Shenyang University of Chemical Technology

*Author for correspondence: wyt_shzu@163.com; jiaxin@shzu.edu.cn；

maleixinjiang@gmail.com

ACCEPTED MANUSCRIPT

Table S1. UV-vis absorption and fluorescence emission wavelength of six compounds at different solvents.

Entry	λ_{max}[a] (nm)	λ_{max}[b] (nm)	FWHM (nm)
PTCDA	573/567/575	601/598/608	37.08/43.06/41.69
m-2MeOPTCDA	571/566/573	605/609/615	35.59/41.46/42.25
t-BuOPTCDA	579/575/581	613/599/617	37.45/35.89/40.29
p-MeOPTCDA	586/567/586	613/599/617	34.72/40.06/50.10
o-MeOPTCDA	584/581/585	609/605/615	33.52/35.22/47.98
m-MeOPTCDA	575/567/575	601/600/608	36.44/39.14/40.46

[a] The maximum absorption wavelength. [b] The maximum emission wavelength. [c] The peak width at half height (FWHM) of maximum emission peaks in different solvents. (left: toluene, middle: THF, right: DMF).

Table S2. The maximum excitation wavelength and fluorescence emission wavelength of six light conversion films.

Entry	λ_{exc}[a] (nm)	λ_{em}[b] (nm)	FWHM[c] (nm)
PTCDA	582	651	48.89
m-2MeOPTCDA	583	647	44.40
t-BuOPTCDA	590	658	50.06
p-MeOPTCDA	609	667	45.24
o-MeOPTCDA	590	657	46.22
m-MeOPTCDA	581	651	45.66

[a] maximum excitation wavelength. [b] maximum emission wavelength. [c] the peak width at half height (FWHM) of maximum emission peaks in PVC film.

Table S3. Light transmittance of light conversion films at different wavelength ranges.

Entry	λ (200-400nm)	λ (400-500nm)	λ (500-600nm)	λ (600-650nm)
PTCDA	47.00%	58.93%	27.22%	89.13%
m-2MeOPTCDA	45.01%	55.50%	26.97%	91.21%
t-BuOPTCDA	46.06%	57.12%	29.07%	29.07%
p-MeOPTCDA	40.92%	47.83%	21.88%	60.80%
o-MeOPTCDA	45.48%	56.84%	23.52%	75.92%
m-MeOPTCDA	45.17%	54.91%	25.43%	89.29%

ACCEPTED MANUSCRIPT

Table S4. Light transmittance of mixed light conversion films at different wavelength ranges (the mass of m-MeOPTCDA:TPA=1:0, 1:1, 1:2, 1:4).

Entry	λ (200-400nm)	λ (400-500nm)	λ (500-600nm)	λ (600-650nm)
1:0	45.17%	54. 91%	25.43%	89.29%
1:1	21.74%	60.26%	29.90%	91.92%
1:2	16.24%	60.13%	30.35%	91.67%
1:4	11.94%	61.67%	31.68%	91.31%

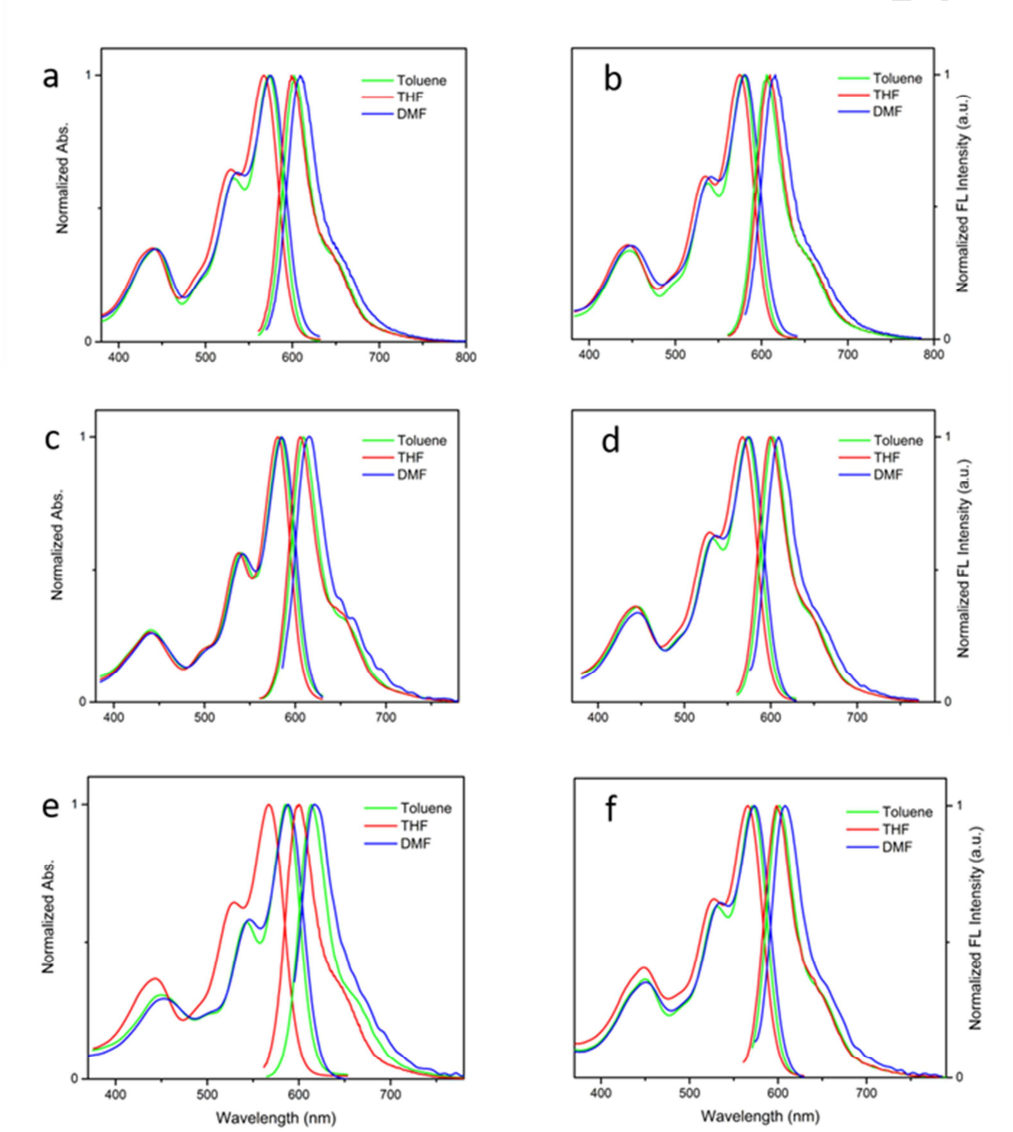

Figure S1 UV-vis absorption and fluorescence emission spectra of PTCDA(a), t-BuOPTCDA(b), o-MeOPTCDA(c), m-MeOPTCDA(d), p-MeOPTCDA(e) and m-2MeOPTCDA(f) in different polar solvents (1×10^{-5} mol/L).

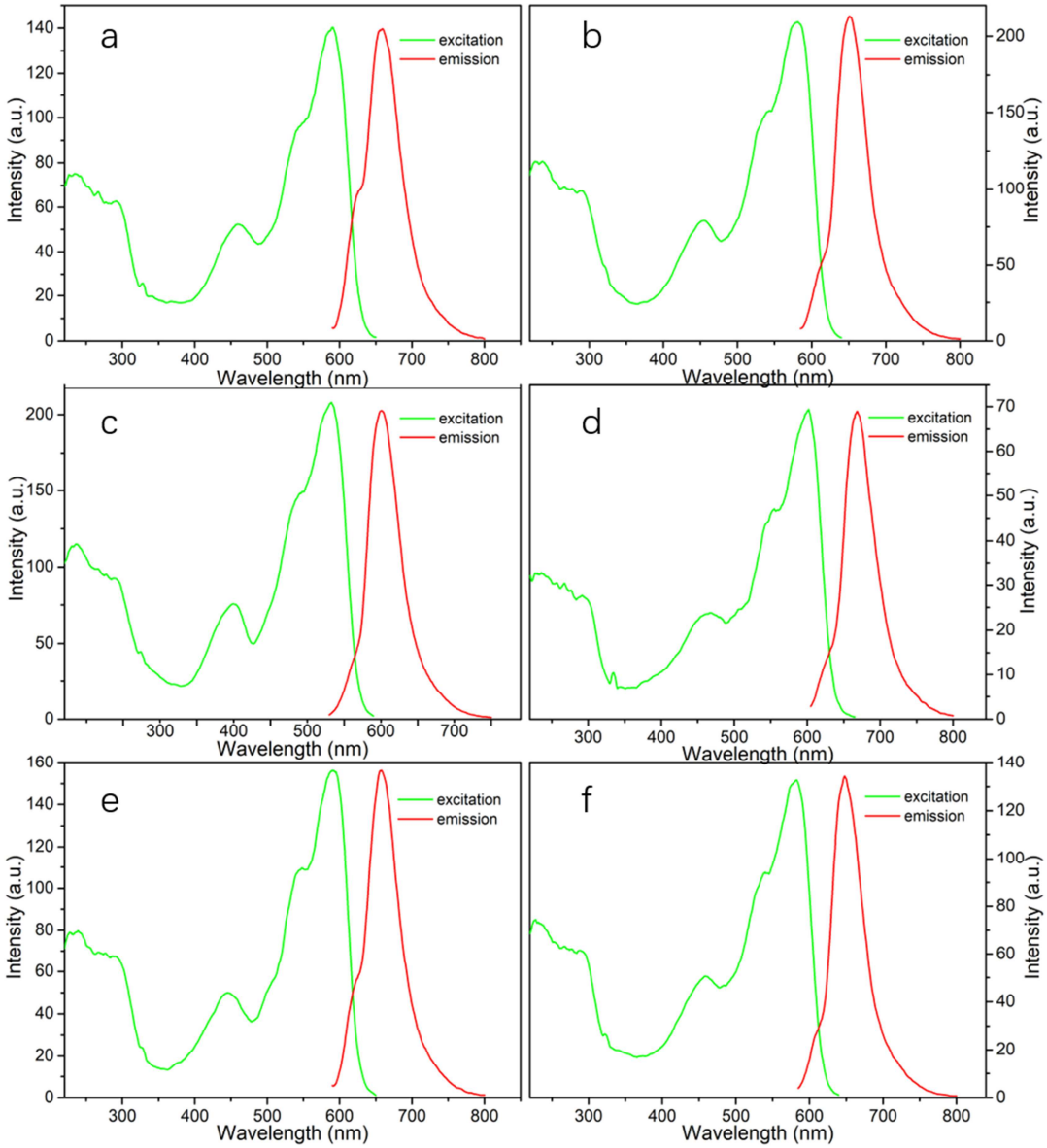

Figure S2. The excitation and emission spectra of t-BuOPTCDA(a), m-MeOPTCDA(b), PTCDA(c), p-MeOPTCDA(d), o-MeOPTCDA(e) and m-2MeOPTCDA(f) in PVC doped films (0.5% addition concentration by weight).

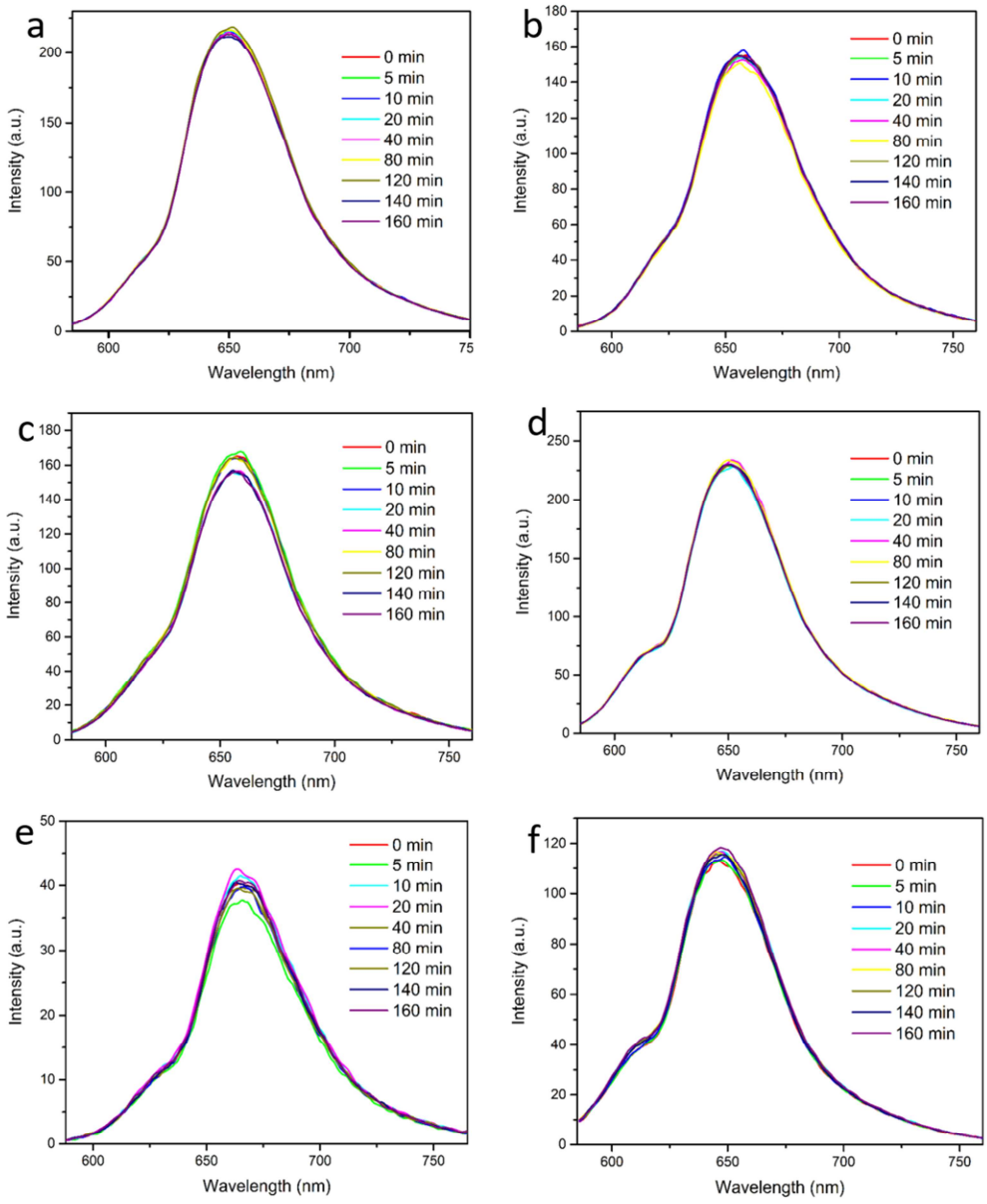

Figure S3 The fluorescence spectra of PTCDA(a), t-BuOPTCDA(b), o-MeOPTCDA(c), m-MeOPTCDA(d), p-MeOPTCDA(e) and m-2MeOPTCDA(f) in PVC films (0.5% addition concentration by weight) under artificial sunlight irradiation at different times.

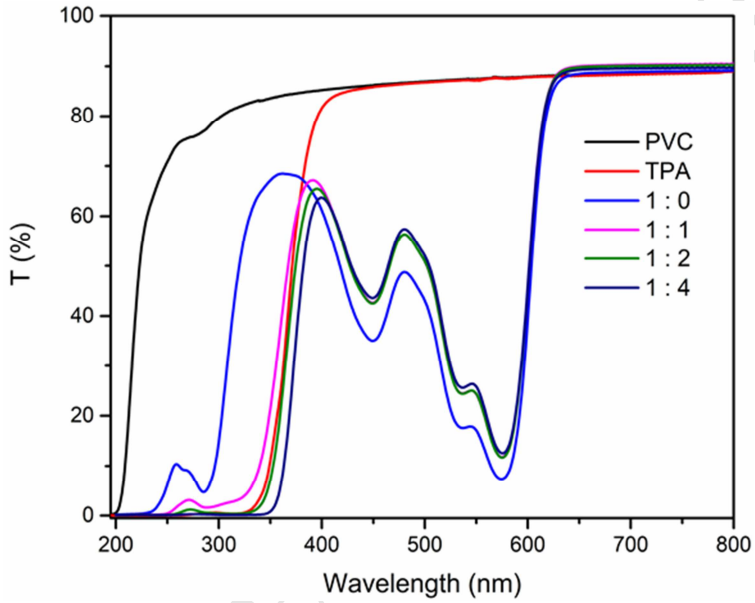

Figure S4 UV-visible transmittance spectra of composite films containing m-MeOPTCDA and TPA depending on different weight ratio(TPA: m-MeOPTCDA=1:0, 1:1, 1:2, 1:4).

ACCEPTED MANUSCRIPT

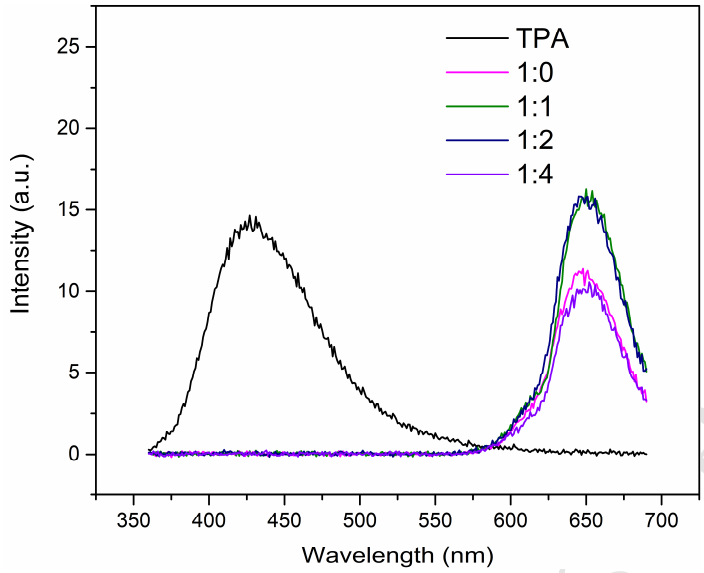

Figure S5. The fluorescence spectra spectra of composite films containing m-MeOPTCDA and TPA according to different adding proportions (λ_{ex}=350 nm).

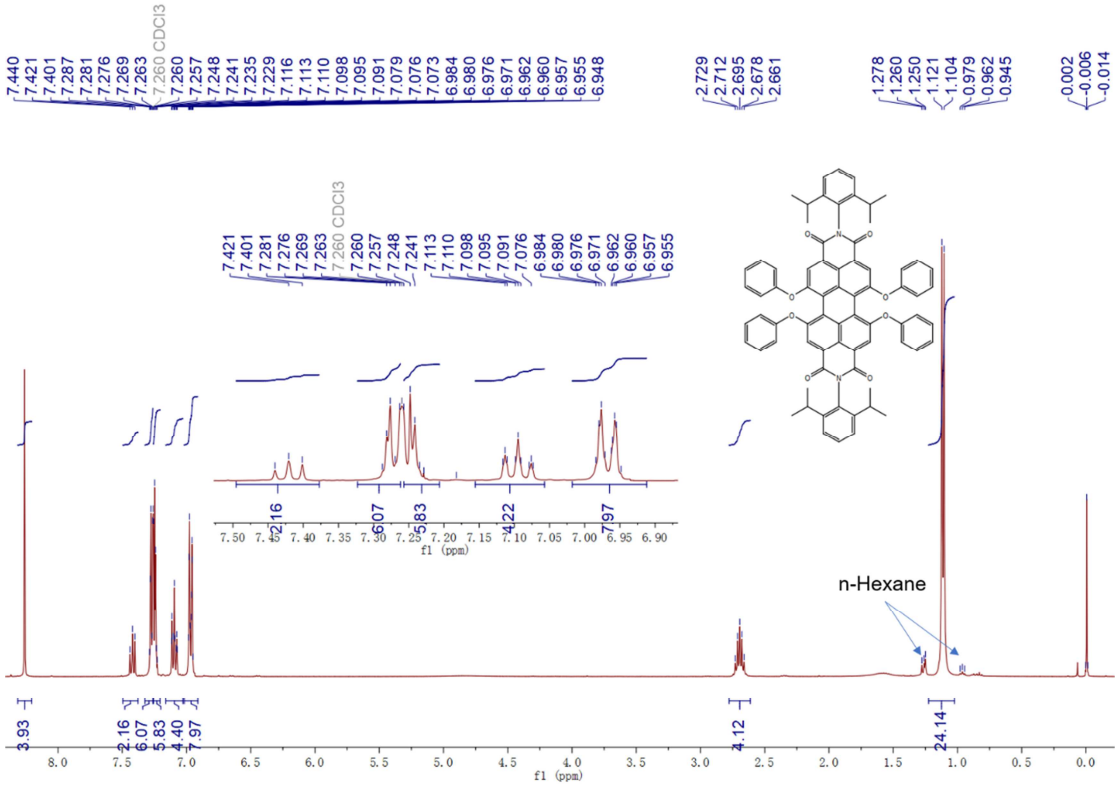

Figure S6. ^{1}H NMR (400MHz) spectrum of PTCDA in $CDCl_3$.

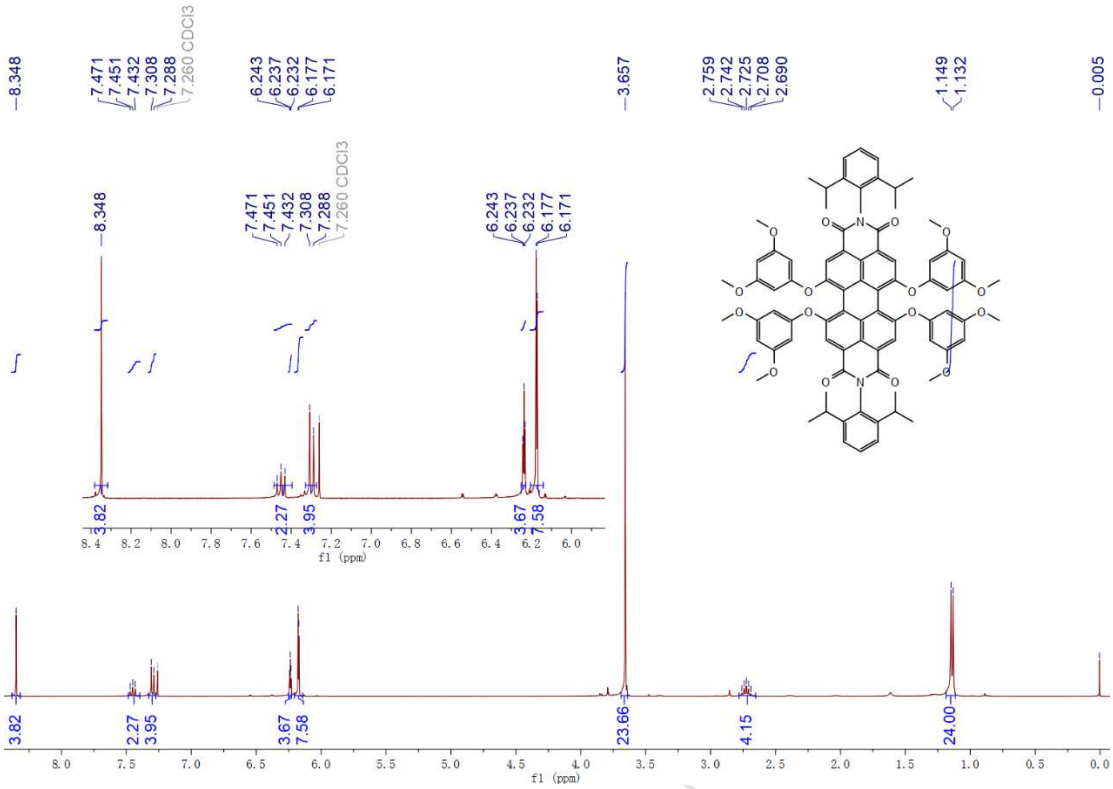

Figure S7. ^{1}H NMR (400MHz) spectrum of m-2MeOPTCDA in $CDCl_3$.

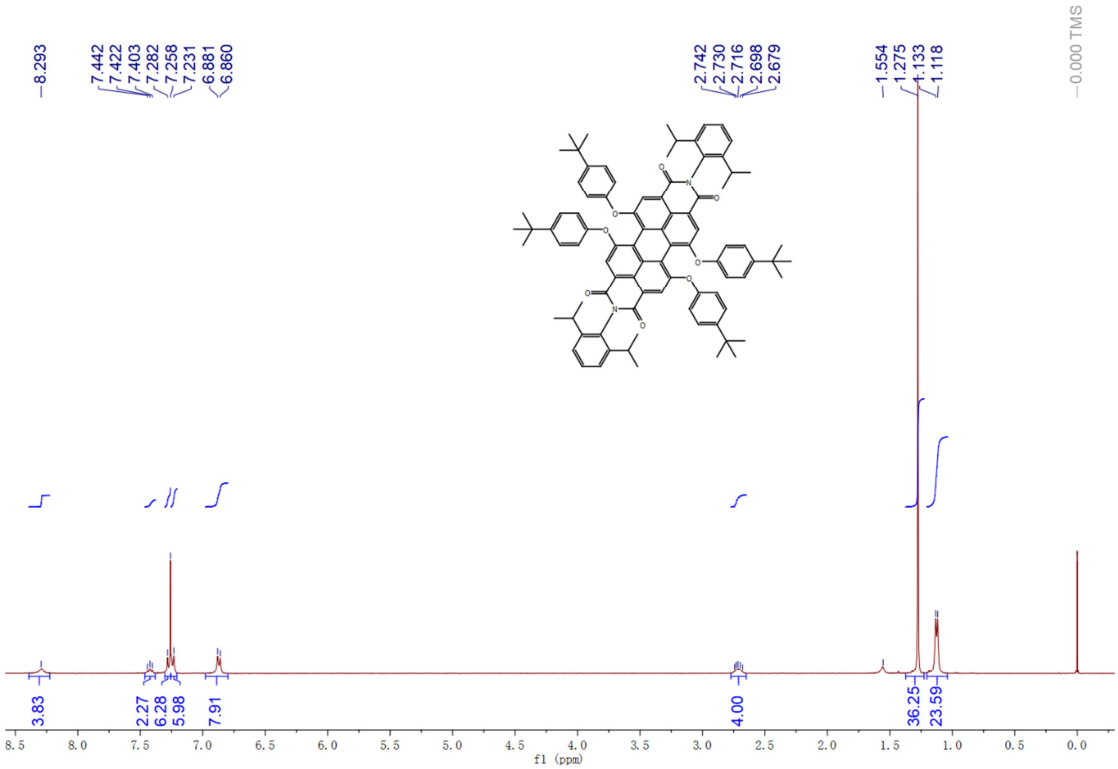

Figure S8. ^{1}H NMR (400MHz) spectrum of t-BuOPTCDA in $CDCl_3$

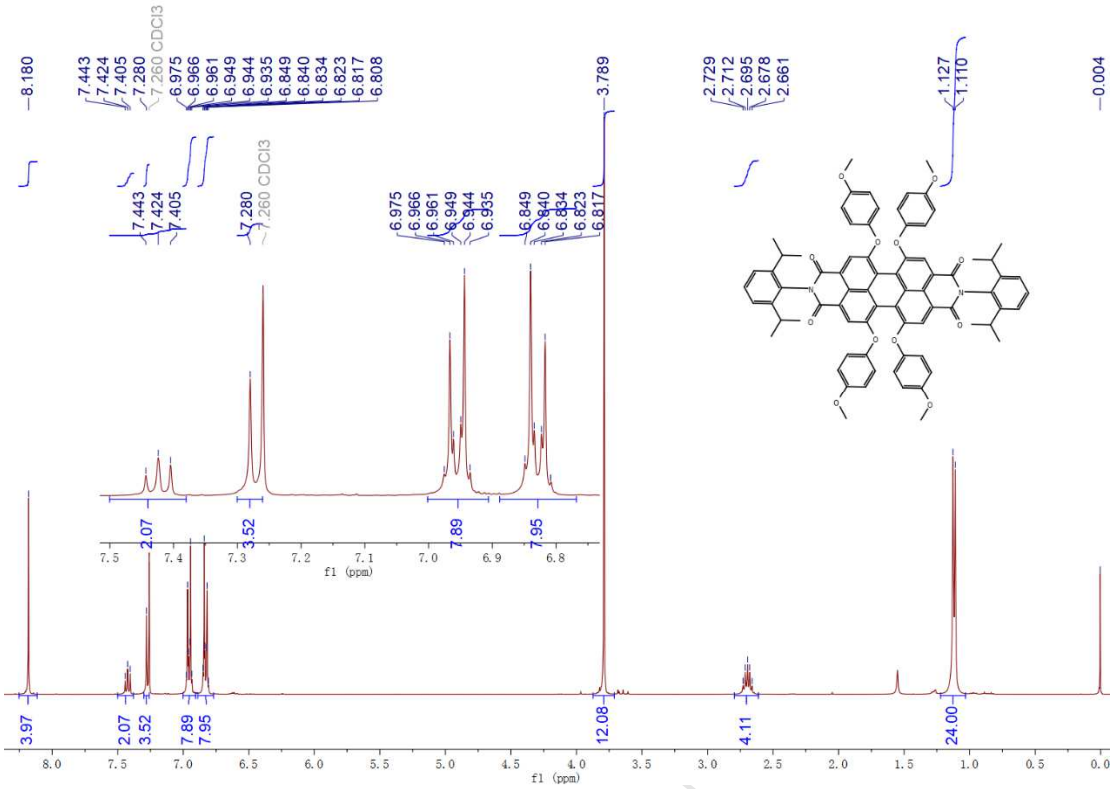

Figure S9. ^{1}H NMR (400MHz) spectrum of p-MeOPTCDA in $CDCl_3$

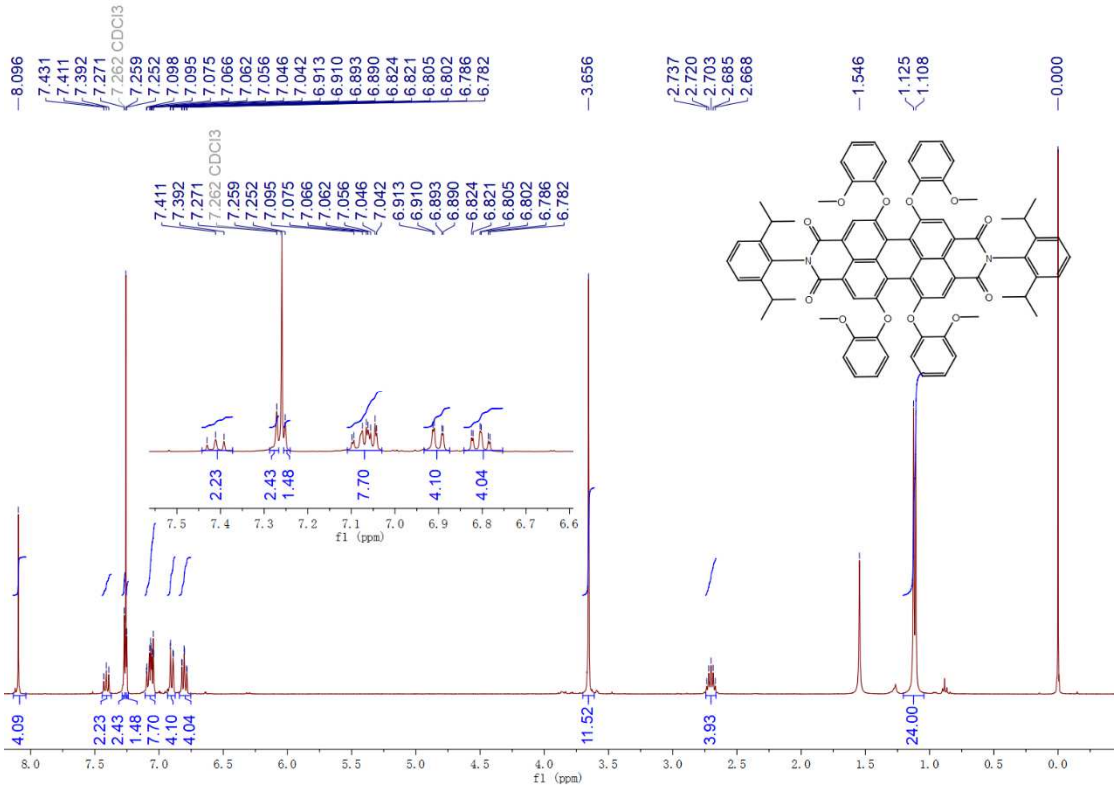

Figure S10. ^{1}H NMR (400MHz) spectrum of o-MeOPTCDA in $CDCl_3$.

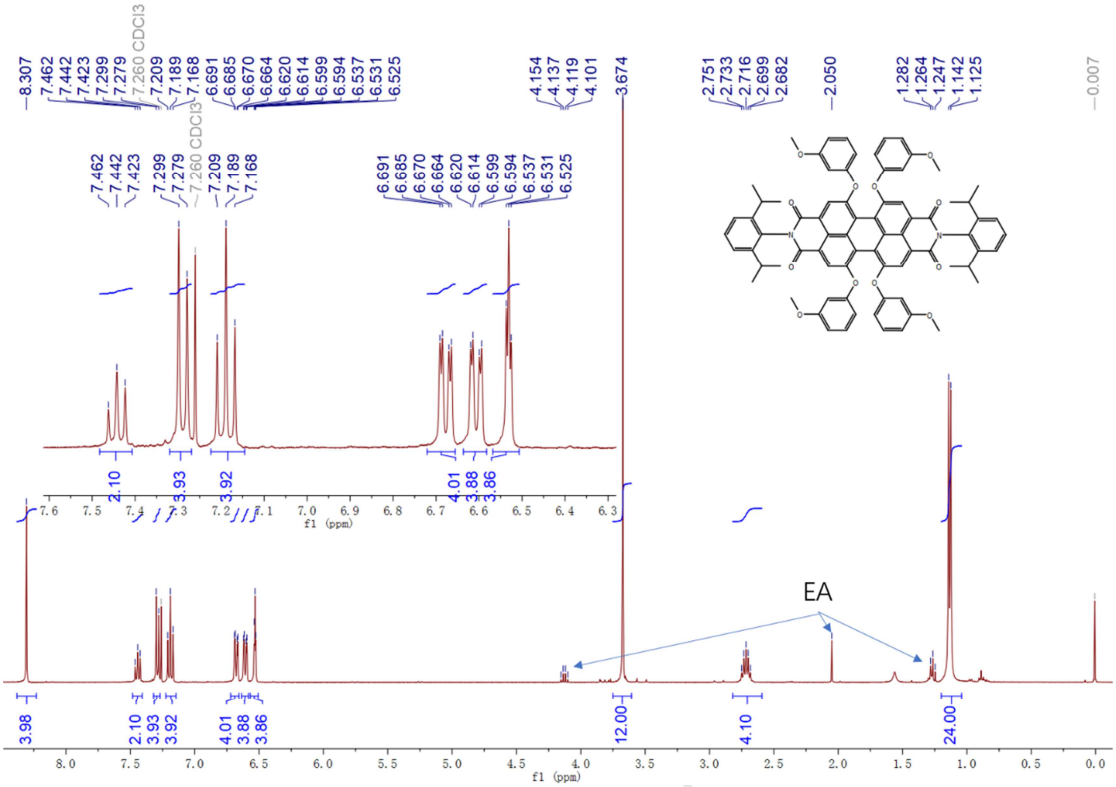

Figure S11. ^{1}H NMR (400MHz) spectrum of m-MeOPTCDA in $CDCl_3$.

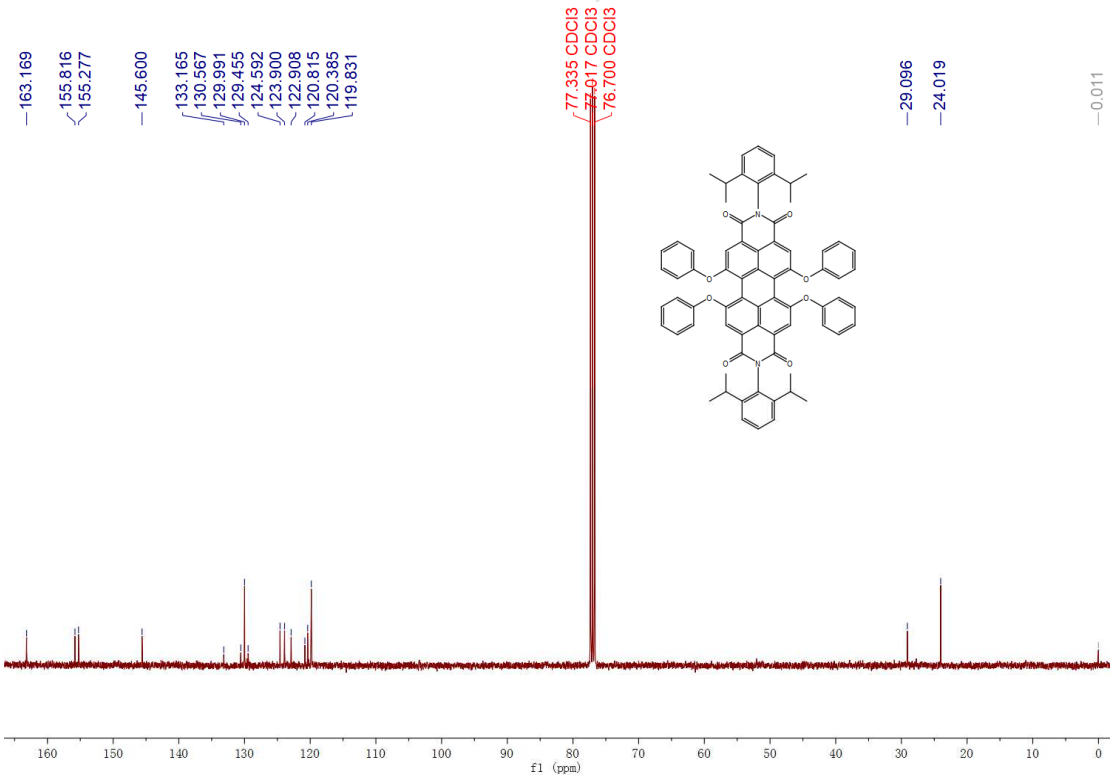

Figure S12. ^{13}C NMR (400MHz) spectrum of PTCDA in $CDCl_3$.

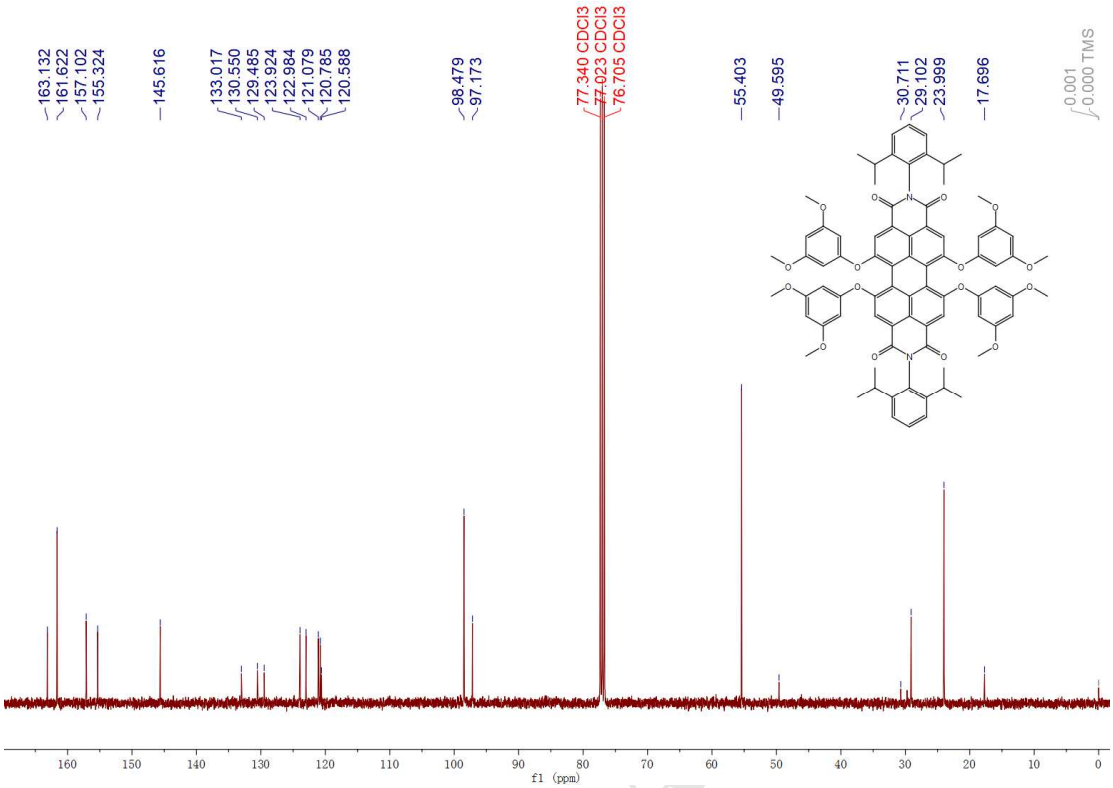

Figure S13. ^{13}C NMR (100MHz) spectrum of m-2MeOPTCDA in $CDCl_3$.

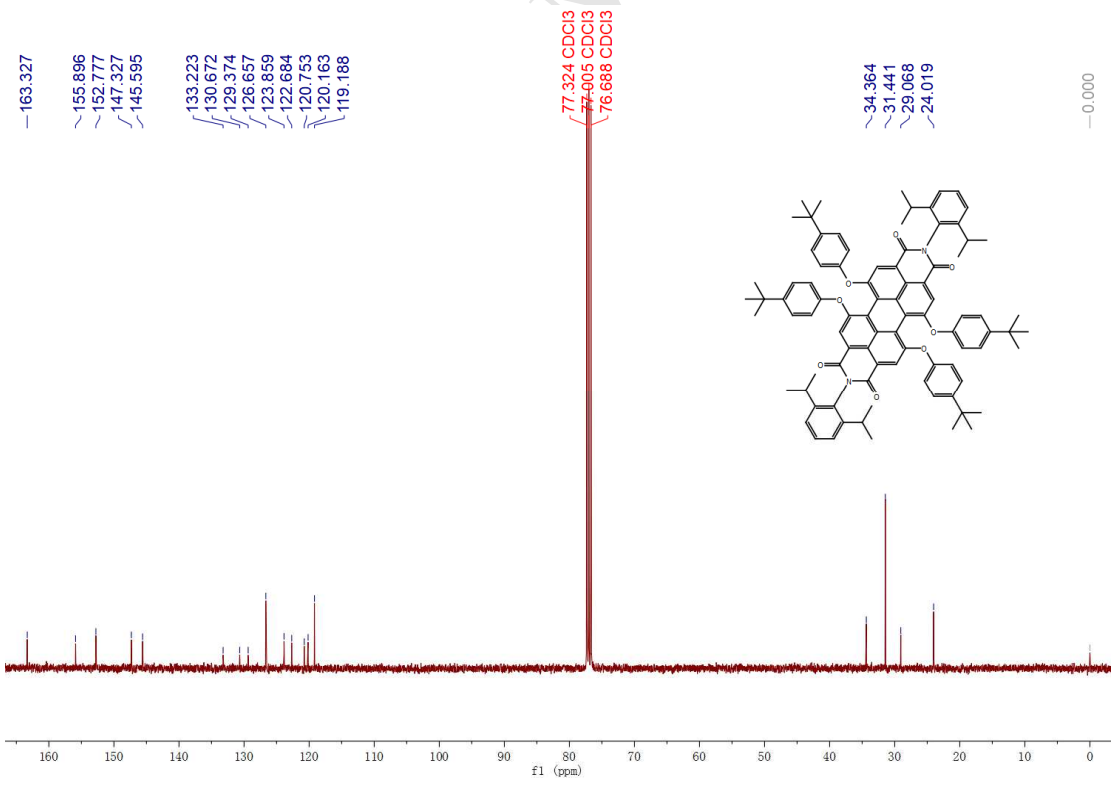

Figure S14. ^{13}C NMR (400MHz) spectrum of t-MeOPTCDA in $CDCl_3$.

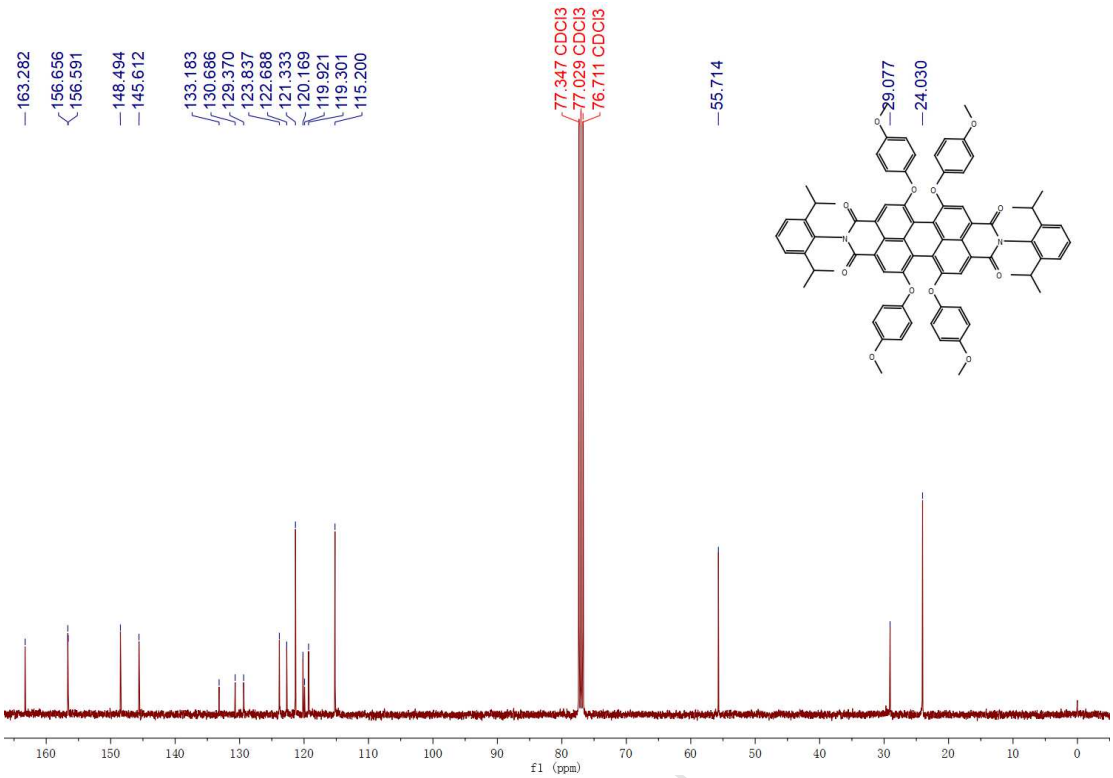

Figure S15. ^{13}C NMR (400MHz) spectrum of p-MeOPTCDA in $CDCl_3$.

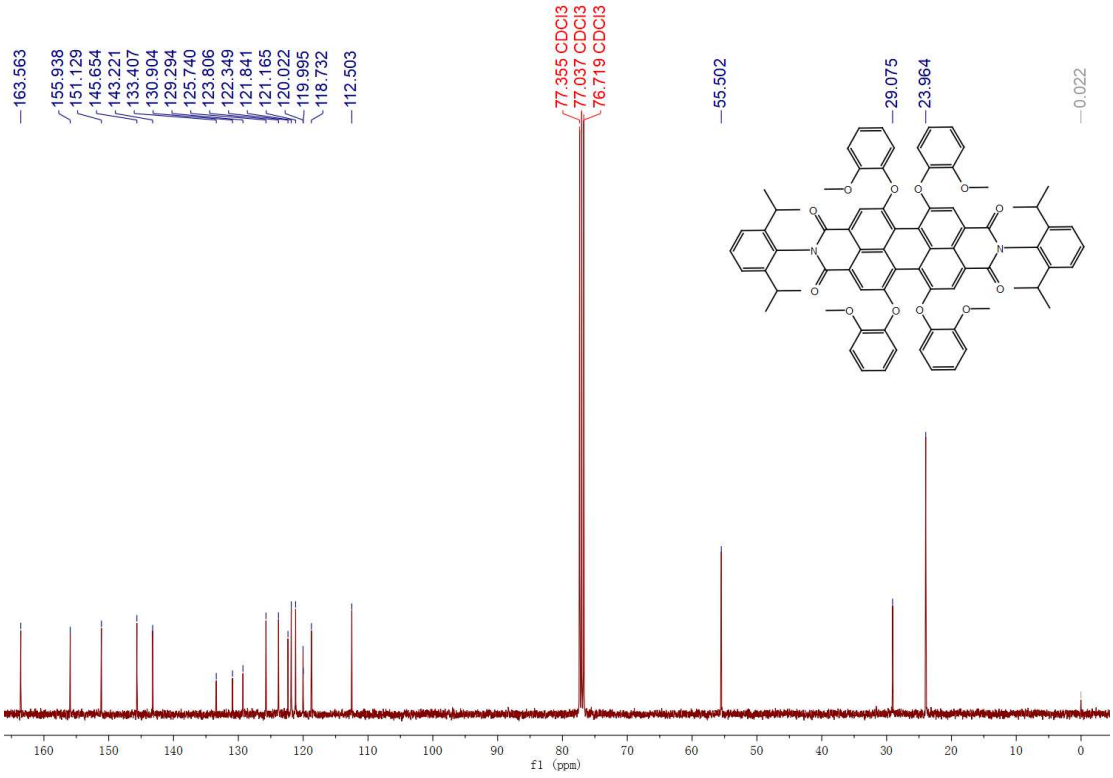

Figure S16. ^{13}C NMR (400MHz) spectrum of o-MeOPTCDA in $CDCl_3$.

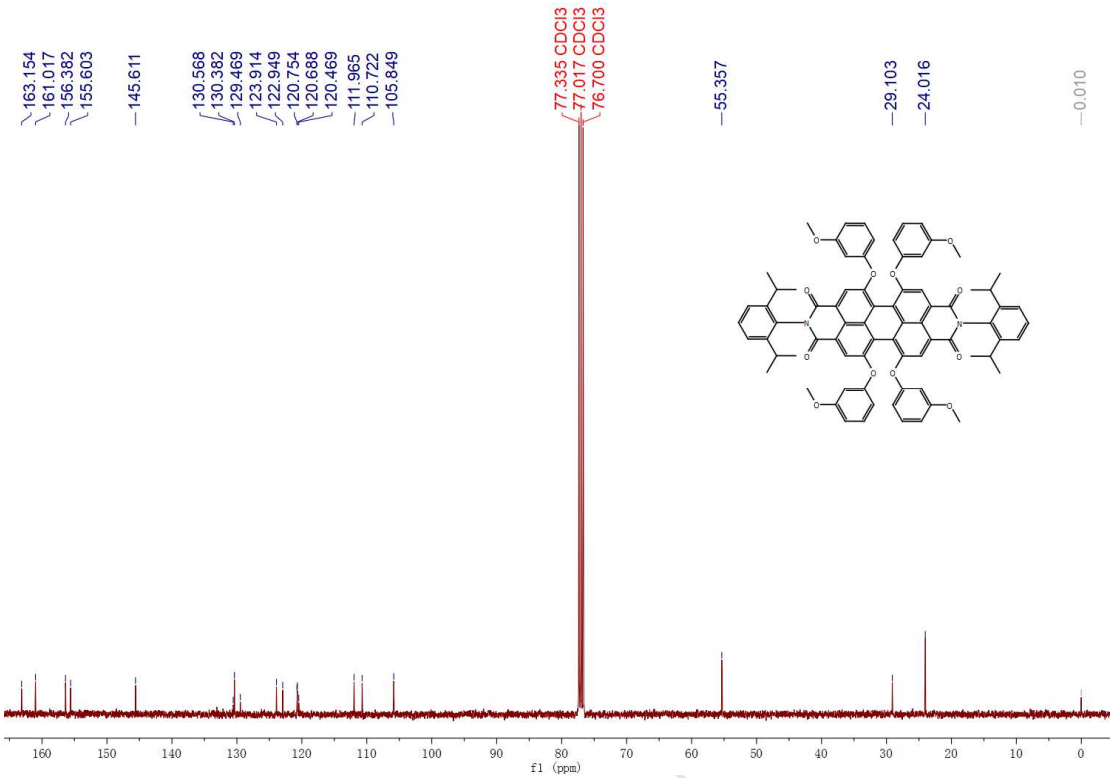

Figure S17. ^{13}C NMR (400MHz) spectrum of m-MeOPTCDA in $CDCl_3$.

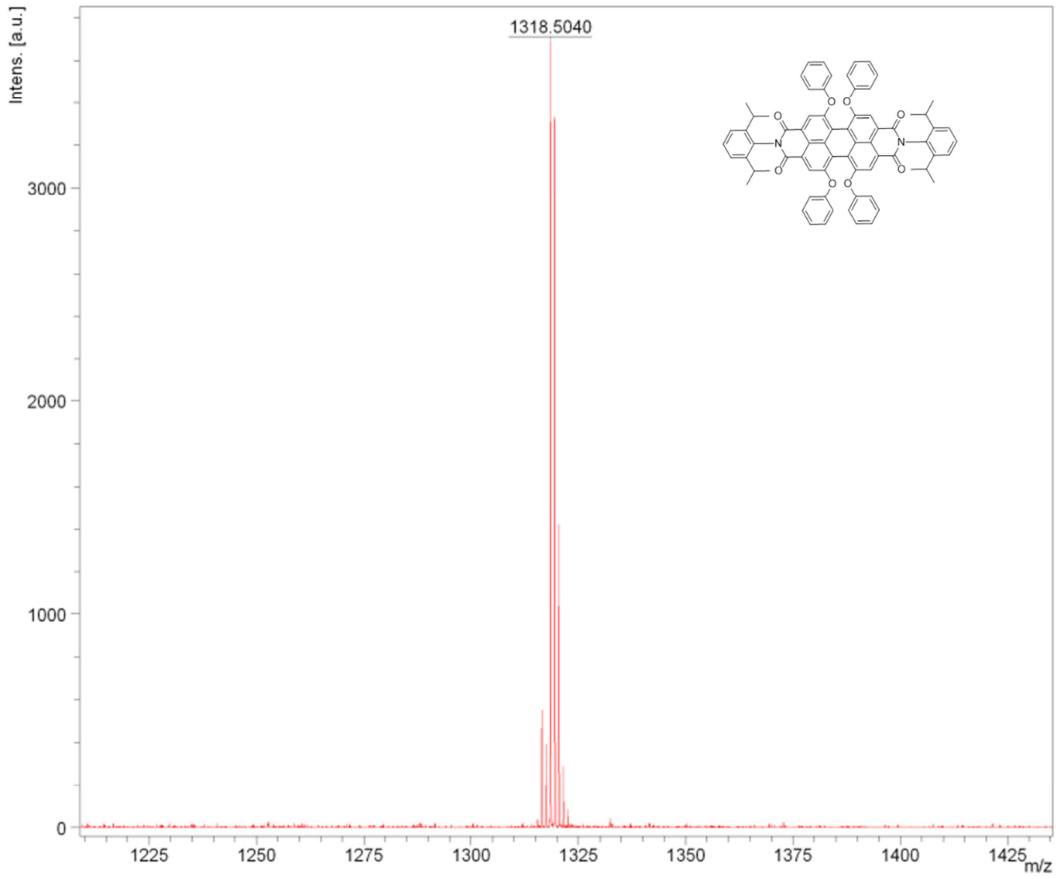

Figure S18. MALDI/TOF MS spectrum of PTCDA.

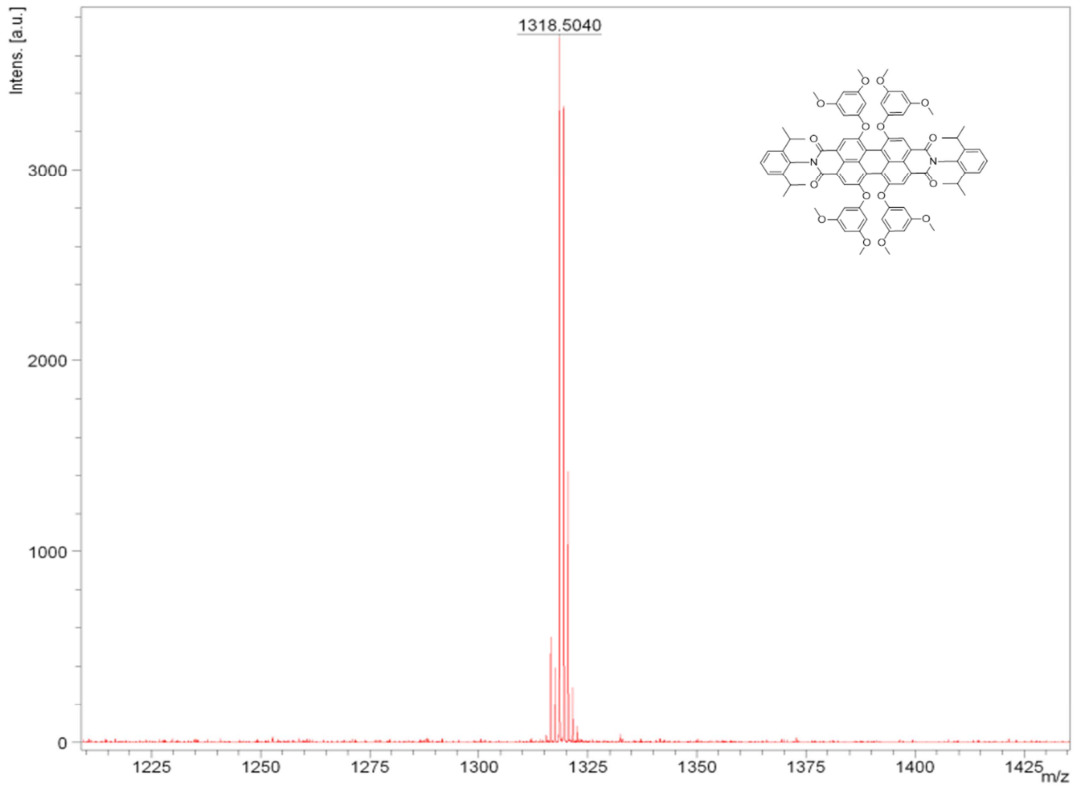

Figure S19. MALDI/TOF MS spectrum of m-2MeOPTCDA.

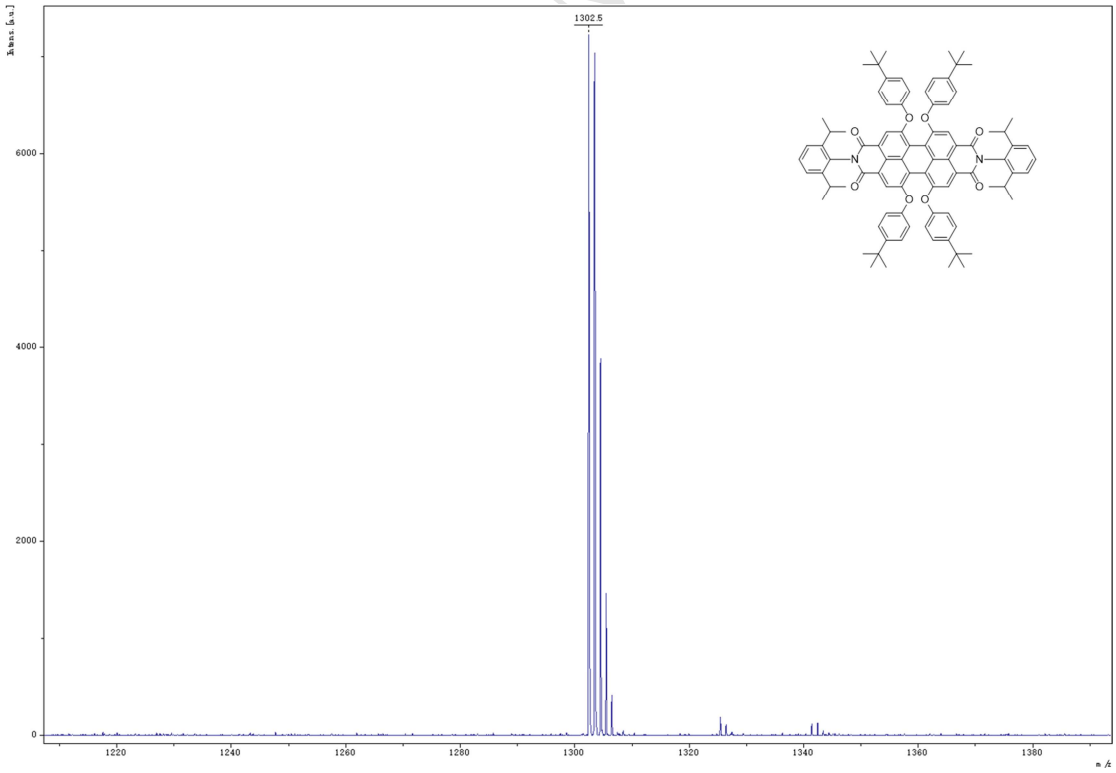

Figure S20. MALDI/TOF MS spectrum of t-BuOPTCDA.

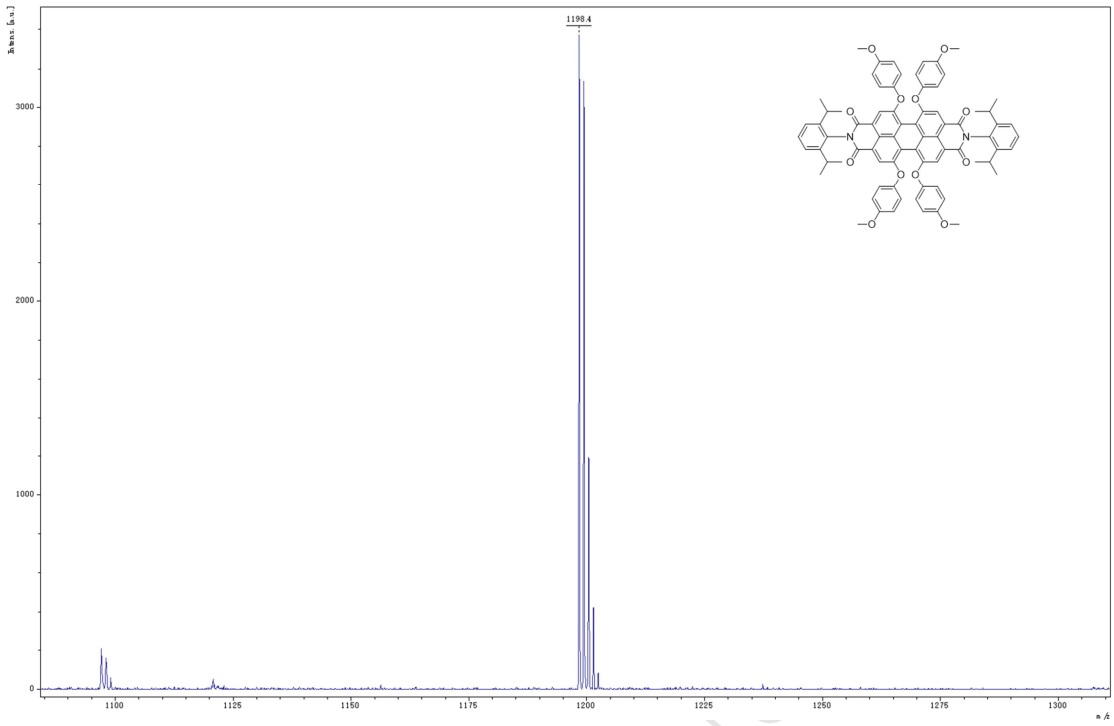

Figure S21. MALDI/TOF MS spectrum of p-MeOPTCDA.

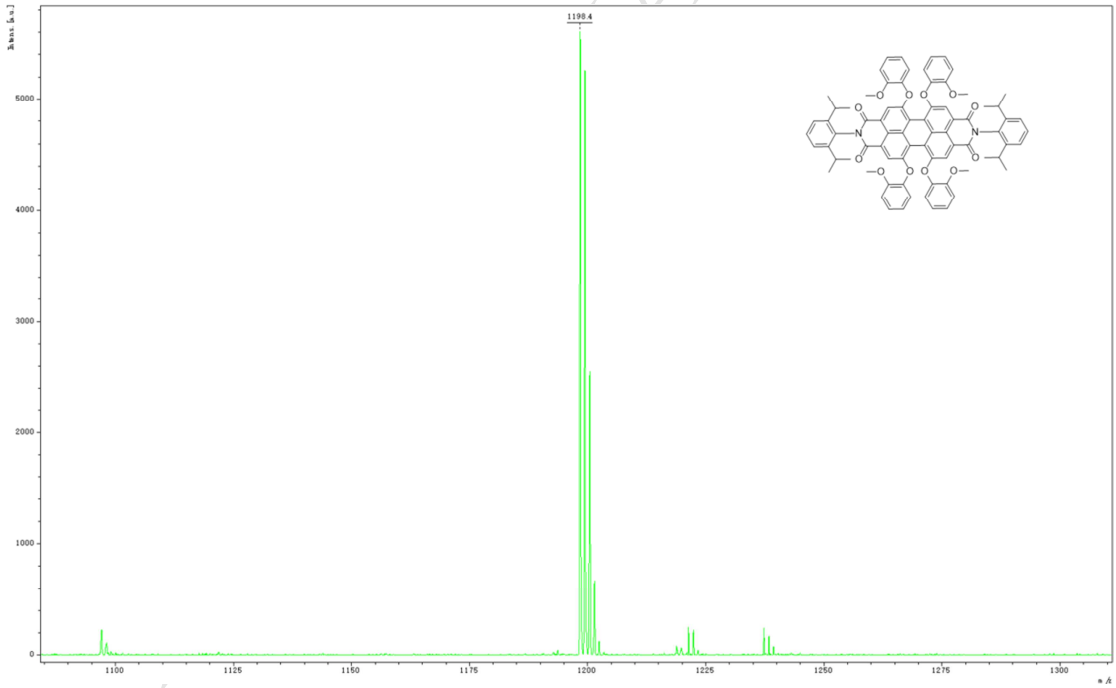

Figure S22. MALDI/TOF MS spectrum of o-MeOPTCDA.

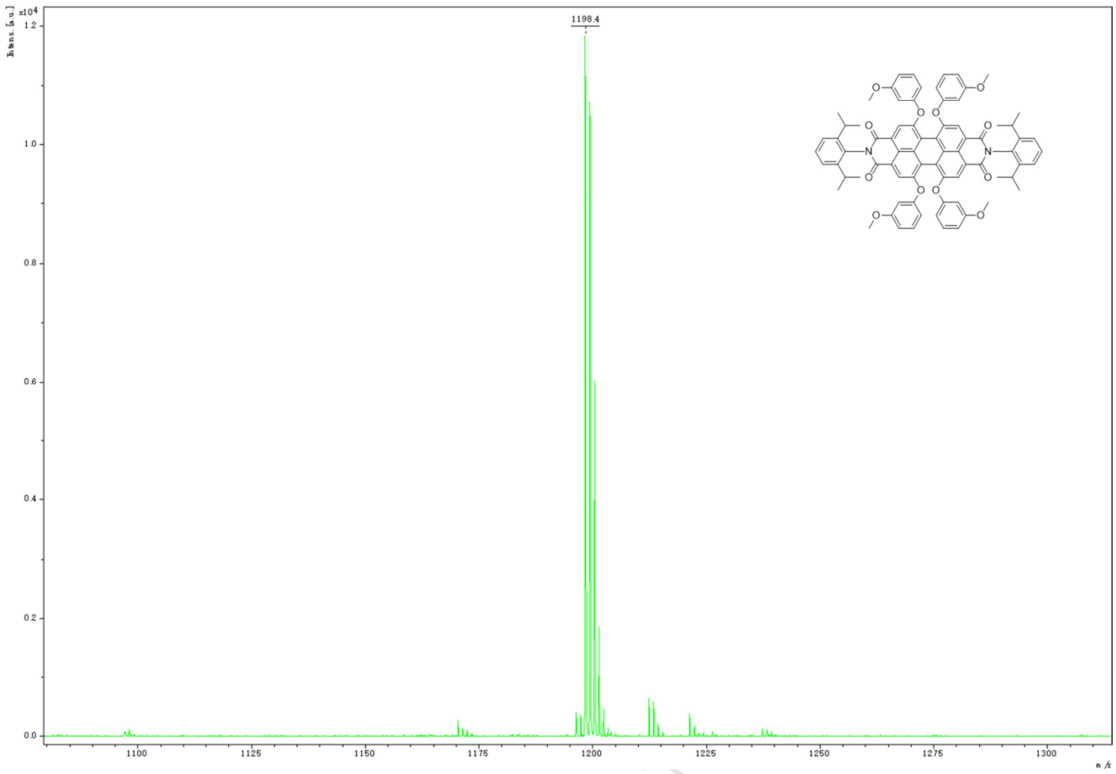

Figure S23. MALDI/TOF MS spectrum of m-MeOPTCDA.

ACCEPTED MANUSCRIPT

ACCEPTED MANUSCRIPT

Highlights

1. As light conversion materials for agricultural film, the application and evaluation of bay-substituted PDI derivatives are investigated in detail.
2. m-MeOPTCDA exhibited matching fluorescence emission with crop absorption in doping film.
3. The fluorescence quantum yields of PTCDA, t-BuOPTCDA and m-MeOPTCDA are up to 0.88, 0.84 and 0.78 in doping films.
4. The m-MeOPTCDA-doped film displays excellent photo-stability after strengthening solar radiation and outdoor exposure to sunlight.
5. The double layer coextrusion film containing m-MeOPTCDA and Triphenyl acrylonitrile is succeed in dual band excitation（350 nm and 580 nm）and emission (430 nm and 651 nm).

ACCEPTED MANUSCRIPT